

University of Memphis

University of Memphis Digital Commons

Electronic Theses and Dissertations

11-25-2019

Sublimation Rate of Paradichlorobenzene Spheres in a Natural Convection Environment

Christopher Bryan Anderson

Follow this and additional works at: <https://digitalcommons.memphis.edu/etd>

Recommended Citation

Anderson, Christopher Bryan, "Sublimation Rate of Paradichlorobenzene Spheres in a Natural Convection Environment" (2019). *Electronic Theses and Dissertations*. 2044.

<https://digitalcommons.memphis.edu/etd/2044>

This Thesis is brought to you for free and open access by University of Memphis Digital Commons. It has been accepted for inclusion in Electronic Theses and Dissertations by an authorized administrator of University of Memphis Digital Commons. For more information, please contact khhgerty@memphis.edu.

SUBLIMATION OF SUSPENDED PARADICHLOROBENZENE SPHERES IN
A NATURAL CONVECTION ENVIRONMENT

by

Christopher B. Anderson

A Thesis

Submitted in Partial Fulfillment of the

Requirements for the Degree of

Master of Science

Major: Mechanical Engineering

The University of Memphis

December 2019

Dedication

I would like to dedicate this work to all the family, friends, and mentors who have supported and helped me along in my academic career. My family have always been there for me through all the hardships and has always been very encouraging. My friends were always there to help me unwind and keep my sanity. A huge gratitude is in order to Dr. Janna for pushing me to do my best and providing me the knowledge required for an advanced degree.

Abstract

Spherical paradichlorobenzene specimens were cast, then allowed to sublime in a natural convection environment. The mass loss over time was recorded, suspending the specimens by a weigh bellow hook attached to a balance, which was required to obtain the sublimation rate. The diameters tested in this study were 3 cm, 4 cm, 5 cm, and 5.8 cm. A total of three data sets for each sized sphere were recorded to ensure accuracy.

The results were used to determine the Schmidt, Grashoff, Sherwood, and Rayleigh numbers. After finding these values, an emperical equation was found relating the Sherwood number as a function of the Rayleigh number. Using this technique and these results it is possible to determine heat transfer coefficients via the heat mass transfer analogy. This method is not only bound to spheres and natural convection, for it can be used to analyze more complex geometries as well as forced convection environments.

Table of Contents

Chapter	Page
List of Tables	iv
List of Figures	v
1. Introduction.....	1
Objective.....	1
Background.....	2
2. Literature Review	3
Applications	3
Cylindrical Geometry	3
Natural Convection	3
Forced Convection.....	8
Spherical Geometry	8
Natural Convection	8
Summary of Literature and Gaps in Knowledge	10
3. Materials and Methods.....	11
Creating Molds.....	11
Casting Specimens	19
Data Acquisition.....	20
Equations	21

Results	26
4. Overall Conclusion	30
Discussion and Conclusion	30
Recommendation for Future Work	31
References	33
Appendix	34

List of Tables

Table 1: Constants used in Bautista calculations.	4
Table 2: Bautista experimental results.	4
Table 3: Constants used for Snapp calculations.	7
Table 4: Snapp experimental results.	7
Table 5: Constants used for W. Anderson calculations.	9
Table 6: W. Anderson experimental results.	9
Table 7: Constants used for calculations.	26
Table 8: Reduced data for 30mm sphere trials.	27
Table 9: Reduced data for 40mm sphere trials.	27
Table 10: Reduced data for 50mm sphere trials.	28
Table 11: Reduced data for 58mm sphere trials.	28

List of Figures

Figure 1:Plot of the Sherwood Number and Rayleigh Number for Butista results.	5
Figure 2:Plot of the Sherwood Number and Rayleigh Number for Snapp results.....	7
Figure 3:Plot of the Sherwood Number and Rayleigh Number for W. Anderson results.	10
Figure 4:First finished mold made from ABS plastic.	11
Figure 5:First casting test in ABS mold which was required to be cut open due to the paradichlorobenzene melting the plastic from a chemical reaction.....	11
Figure 6:Spherical silicone baking molds purchased online.....	12
Figure 7:Pictured above, un-altered 3d printed mold negative on the left and acetone vapor smoothed mold negative on the right.....	12
Figure 8:Technical drawing of the lower half mold negative used to create the lower silicone mold.	13
Figure 9:Technical drawing of the upper half mold negative used to create the upper silicone mold.	14
Figure 10:Cutaway view of the plastic mold negative and silicone retainer assembled.	14
Figure 11:The silicone being poured into mold negatives.....	15
Figure 12:The silicone two-part component initially poured into mixing cup on the left and the thoroughly mixed silicone on the right.	15
Figure 13:Mold negatives assembled, cleaned and ready to accept silicone.....	15
Figure 14:Silicone cured, and the mold negative is ready for disassembling.	16
Figure 15:Center post removed, revealing a fill hole.....	16
Figure 16:Removing the silicone retainer ring.	17
Figure 17:Silicone mold removed from mold negative.....	17

Figure 18:All components disassembled revealing the two silicone mold halves, ready to be used. 18

Figure 19:From left to right, the sewing needle with fishing line is fed from the inside of the mold and out through the top. The line is pulled through until the melted end of the line is even with the surface of the flange on the mold, placing the line in the center of the finished specimen. 19

Figure 20:The tip at one end of the fishing line was melted, creating a small ball, to prevent the line from coming out of the cast specimen..... 19

Figure 21:Assembled mold placed on transportation tray with thermal insulation pad..... 20

Figure 22:Melting paradichlorobenzene moth balls in stainless-steel dish on electric skillet. 20

Figure 23:Pouring melted paradichlorobenzene into silicone mold. 20

Figure 24: Specimen hung on the weigh below hook and ready for starting mass data acquisition. 21

Figure 25: Mold separated, specimen removed, then trimmed fill plug excess, and tied a loop in the string for suspending 21

Figure 26: When $r=R$ the vapor density is equal to C_A . At a far distance, as $r \rightarrow \infty$, $C_\infty = 0$... 24

Figure 27: Reduced data results plotting Sherwood number versus Rayleigh number..... 29

Figure 28: Experimental mass transfer rate plotted for trial 1. 34

Figure 29: Experimental mass transfer rate plotted for trial 2. 35

Figure 30: Experimental mass transfer rate plotted for trial 3. 36

Figure 31: Experimental mass transfer rate plotted for trial 4. 37

Figure 32: Experimental mass transfer rate plotted for trial 5. 38

Figure 33: Experimental mass transfer rate plotted for trial 6. 39

Figure 34: Experimental mass transfer rate plotted for trial 7.	40
Figure 35: Experimental mass transfer rate plotted for trial 8.	41
Figure 36: Experimental mass transfer rate plotted for trial 9.	42
Figure 37: Experimental mass transfer rate plotted for trial 10.	43
Figure 38: Experimental mass transfer rate plotted for trial 11.	44
Figure 39: Experimental mass transfer rate plotted for trial 12.	45

Introduction

The technique of paradichlorobenzene sublimation is an experimental method used to ultimately determine heat transfer convection coefficients. The main characteristic of this method is to model a specific heat transfer problem by creating an analogous relationship to an identical mass transfer problem [1]. This method can include but not be limited to forced or free convection and different geometries, such as plates, cylinders, spheres, single fins, or fin arrays to name a few. The two most common materials used in this technique is paradichlorobenzene and naphthalene. Paradichlorobenzene is a relatively easy material to work with making it simple to cast and sublimates at room temperature. This research has relatively recently become useful in electronics applications where a heat sink or an array of components in varying geometries is required to be analyzed in cooling performance.

Objective

It is the objective of this research to derive an empirical equation for determining the mass transfer coefficient of suspended spherical paradichlorobenzene specimens sublimating in a natural convection environment. The aim of this research is to acquire mass transfer rates of different diameter spheres and determine a relationship between the Sherwood, Grashof, Schmidt, and Rayleigh numbers. The Sherwood number in mass transfer is analogous to the Nusselt number in heat transfer. Also, with the results found in this research, a relationship between mass transfer rate and surface area will be determined. There has not been thorough research performed in the sublimation techniques of spherical geometry in natural convection in the past from any findings.

Background

Convective mass transfer is defined as the transport of material between a boundary surface and a moving fluid or between two immiscible moving fluids separated by a mobile interface. [5] There are two types of convection, forced and natural. Natural convection currents develop if there is any variation in density within the fluid phase. Fick's first law has a large role in making this study possible and is stated as $N_A = -D_{AB} \frac{\partial C_A}{\partial r}$, assuming equimolar counter diffusion [2]. This equation describes mass flux, N_A , which is defined as the rate of mass flow per unit area, using a concentration gradient, radius, and diffusion coefficient.

Certain dimensionless numbers prove to be useful in this area of study as well. The Sherwood number is a dimensionless number commonly used to describe the ratio of molecular mass transport resistance to the convective mass transport resistance of the fluid. [5] The Sherwood number is expressed as $Sh = hL/D$, where L is a characteristic length, h is the convective mass transfer film coefficient, and D is the mass diffusivity. Convective heat transfer is similar, but instead is the mode of heat transfer associated with fluid motion. Likewise, the Nusselt number is a dimensionless number commonly used to describe the ratio of convective to conductive heat transfer across a boundary. The Nusselt number is expressed as $Nu = hL/k$, where L is a characteristic length, h is the convective heat transfer coefficient, and k is the thermal conductivity of the fluid.

Literature Review

Applications

This research has recently begun to be used by thermal engineers to evaluate electronic packaging. A large portion of electronic packaging continues to consist of card-on-board configurations [3]. These circuit boards consist of many components in varying geometries and each component has its own convective transfer. Currently, to evaluate a board as a whole requires an exorbitant amount of time. The data from studies, such as this one, can greatly reduce the time required to develop electronic circuit boards. Likewise, this method could be used to determine convection performance in heatsinks.

Cylindrical Geometry

Natural Convection

This method of using mass transfer results to relate heat transfer has been used previously in the past. One of the more recent studies was performed by Karyn M. Bautista (2010) [4] in which she evaluated the cylindrical geometry in horizontal orientation in a natural convection environment. These experiments were performed using 99.8% paradichlorobenzene [4]. The specimens were created by melting the media using a stainless-steel pan and hot plate and pouring it into molds, which were machined from aluminum, creating a cast. The cylinders cast and used in this study were 1, 1.5, and 2 inches in diameter and 10 inches in length and were cast with a wood skewer through the center of the specimen which was used for suspending. The specimen's mass was measured by the use of a scale equipped with a weigh-below hook and measure to the nearest 0.05 grams with an accuracy of ± 0.02 grams. The mass measurements were recorded, and data logged by a PC connected to the scale using a Visual Basic program [4].

The mass loss over time was graphed and a linear curve fit was used to calculate the mass transfer rate. The specimen's diameter was periodically measured, in three specific locations, throughout the trials and when the diameter reduced by 0.1 inch from its initial measurement, at any location, the trial was terminated. There were several assumptions made to make a conclusion to the study. First, the concentration of paradichlorobenzene is zero far from the sample, which is due to the testing environment being very large [4]. Next, it can be said there is incompressible, isothermal flow at the surface of the specimen where the boundary layer begins [4]. Then, it is assumed chemical reactions are not taking place. Lastly, the paradichlorobenzene vapor properties are constant allowing it to be treated as an ideal gas [4].

The constants used, some found with experimental data and some pre-determined, are shown in Table 1 below [4]. Table 2 shows the experimental results along with the Sherwood, Grashof, and Rayleigh numbers calculated for the different size cylinders tested [4]. The final results in this study yielded an equation of $Sh = 2 \times 10^{-4} \cdot Ra + 2.385$ correlating the data with $R^2 = 0.9999$ [4]. Figure 1 plots the results of the Sherwood numbers and Rayleigh numbers found, giving this equation [4].

Table 1: Constants used in Bautista calculations.

Ambient Temperature, T_w	Gas Constant, R_v	Cylinder length, L	Diffusion Coefficient, D_{AB}	Schmidt number
79°F = 539°R	56.55 J/(kg·K)	0.254 m (= 10 in)	$4.13 \times 10^{-06} \text{ m}^2/\text{s}$	2.23
ρ_v	ρ_v	ρ_{air}	v_{air}	μ_{air}
236.5 Pa	0.009964 kg/m ³	1.265 kg/m ³	$1.41 \times 10^{-5} \text{ m}^2/\text{s}$	$1.79 \times 10^5 \text{ N}\cdot\text{s}/\text{m}^2$

Table 2: Bautista experimental results.

	1 inch	1.5 inch	2 inch
Sublimation rate, kg/s	1.53×10^{-7}	3.40×10^{-7}	6.90×10^{-7}
Diameter, m	0.0254	0.0381	0.0508

Table 2 Continued.

	1 inch	1.5 inch	2 inch
Surface area, m ²	0.02027	0.03040	0.04054
h_m , m/s	0.000757	0.001122	0.001708
Sherwood number	4.7	10.4	21
Grashof number	6 353	21 443	50 828
Rayleigh number	14 169	47 819	113 348

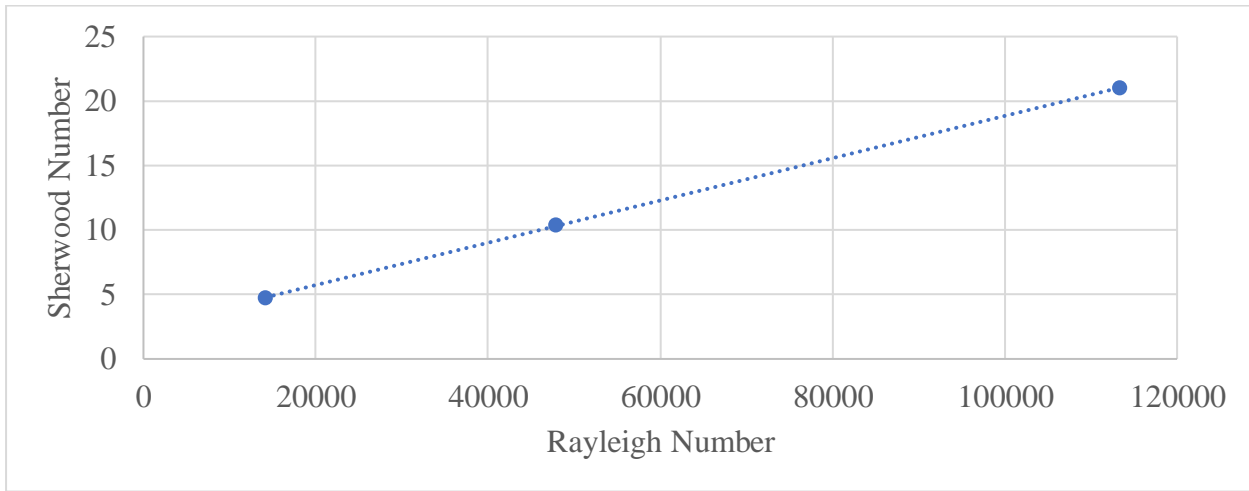


Figure 1: Plot of the Sherwood Number and Rayleigh Number for Butista results.

Another past study was performed by William Snapp (2006) [5], which also evaluated the mass transfer rate of cylindrical geometry in a natural convection environment. The difference in his testing was the orientation of the cylinders being tested, orienting his cylinders in a vertical direction. This study used paradichlorobenzene of 99.8% purity for experimental specimens [5]. These specimens were created by casting paradichlorobenzene in multi piece aluminum molds. The nominal diameters of the molds used were 1, 1.5, and 2 inches by 10 inches in length. The molds were wiped down with alcohol prior to each use and paraffin wax plugs were used to seal the mold to prevent any losses while cooling [5]. The paradichlorobenzene was melted in a stainless-steel pan on a hot plate set to around 170°F before pouring into the mold. The

specimens were solid and ready to be removed after approximately 4 hours. Throughout the study, a total of seven test specimens had to be recast due to defects and imperfections due to flash cooling. After so many unacceptable specimens, Snapp found a solution to the flash cooling by slightly preheating the mold before casting. The mass transfer rates were found by the use of a computer connected to an Ohaus Adventurer scale equipped with a weigh-below hook. The scale used was calibrated to a reported accuracy of ± 0.02 g before used and read to the nearest 0.05 g. The mass, time, date, and trial number were recorded automatically using a program written in Visual Basic. The cylinders cross sectional area was measured periodically by the use of outside calipers at three different locations. The experiment was terminated when the diameter at any location reduced by 0.1 inch from the initial measurement [5].

After the data were collected it was plotted graphically with time on the horizontal axis and mass on the vertical axis. With this, a linear curve fit was performed to find the mass transfer rate [5]. Snapp [5] observed slight fluctuations in the graphs and attributed them to air movement during ventilation in the lab. There were four assumptions made which were necessary to make a conclusion to the study. First, the concentration of paradichlorobenzene is zero far from the sample, which is due to the testing facility used was 160,000 cubic feet [5]. Then, it can be said there is incompressible, isothermal flow at the surface of the specimen where the boundary layer begins [5]. Next, it was assumed chemical reactions are not taking place. Lastly, the paradichlorobenzene vapor properties are constant allowing it to be treated as an ideal gas [5].

The constants used, some found with experimental data and some pre-determined, are shown in Table 3 below [5]. Table 4 shows the sublimation rate results along with the Sherwood, Grashof, and Rayleigh numbers calculated for each size cylinder tested [5]. These results yielded an equation of $Sh = 3 \times 10^{-5} \cdot Ra + 22.53$ correlating the data with $R^2 = 0.9974$ [5]. Figure 2 plots

the results of the Sherwood numbers and Rayleigh numbers found, giving this equation [5]. The differences between the results of Bautista and Snapp alone show that orientation of the specimen affects the outcome of the Sherwood number.

Table 3: Constants used for Snapp calculations.

Ambient Temperature, T_w	Gas Constant, R_v	Cylinder length, L	Diffusion Coefficient, D_{AB}	Schmidt number
79°F = 539°R	56.55 J/(kg·K)	0.254 m = 10 in	$4.13 \times 10^{-6} \text{ m}^2/\text{s}$	2.23
ρ_v	ρ_v	ρ_{air}	ν_{air}	μ_{air}
236.5 Pa	0.009964 kg/m ³	1.265 kg/m ³	$1.41 \times 10^{-5} \text{ m}^2/\text{s}$	$1.79 \times 10^{-5} \text{ N}\cdot\text{s}/\text{m}^2$

Table 4: Snapp experimental results.

	1 inch	1.5 inch	2 inch
Sublimation rate, kg/s	7.56×10^{-7}	7.85×10^{-7}	8.5×10^{-7}
Diameter, m	0.0254	0.0381	0.0508
Surface area, m ²	0.02027	0.0304	0.04054
h_m , m/s	0.003744	0.002591	0.002116
Sherwood number	23	23.9	26
Grashof number	6 353	21 443	50 828
Rayleigh number	14 169	47 819	113 348

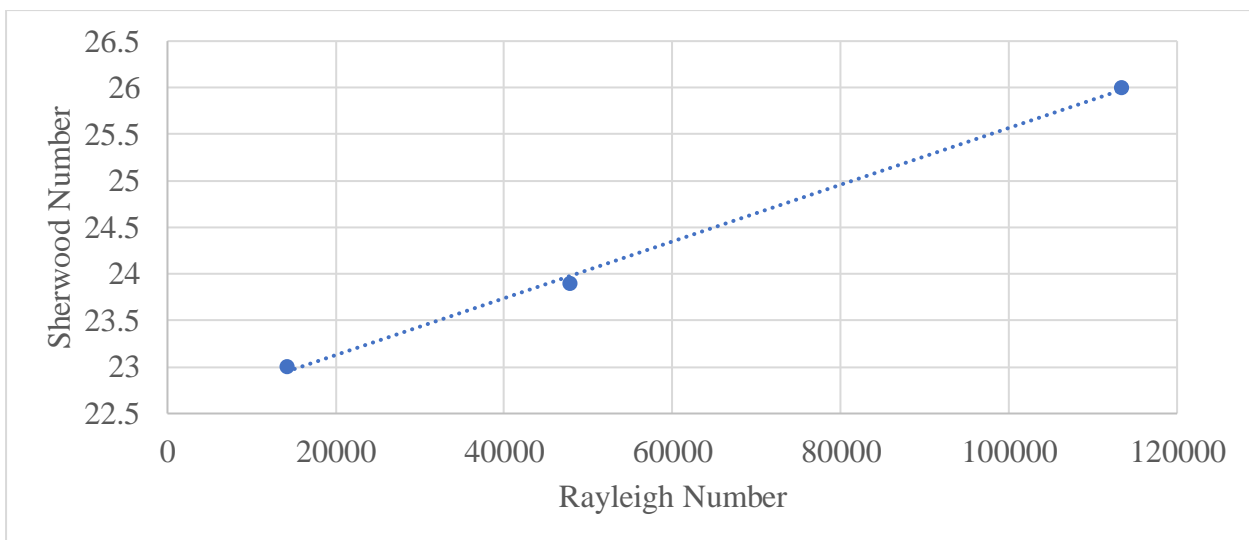


Figure 2: Plot of the Sherwood Number and Rayleigh Number for Snapp results.

Forced Convection

Larry Fite (1991) [6] studied forced convection mass transfer of naphthalene cylinders. The cylinders used in this testing were one, two, and three inches in diameter and 18 inches in length and tested in the horizontal orientation. These specimens were solid naphthalene and created by the use of multipiece aluminum molds. Fite did use PAM™ as a mold release agent in his molds. The specimens were allowed to sublime in an open-loop wind tunnel, exposed to a crossflow of air, for 30–90 minutes [6]. The cylinders were subjected to flows resulting in Reynolds numbers, based on diameter, ranging from 4,700 to 141,000 and velocities from 3 to 30m/s [6].

When forced convection is being analyzed in sublimation, Reynolds number is used instead of the Rayleigh number to evaluate the data. Fite used the results to create a correlation between the average Sherwood number and range of Reynolds numbers. This study resulted in an equation of the Sherwood number in terms of Reynolds number giving $Sh = 0.424 \cdot Re^{0.592}$. The results from this study correlated well with existing heat transfer results when utilizing the heat-mass transfer analogy, with an average uncertainty of $\pm 9.7\%$.

Spherical Geometry

Natural Convection

William Anderson (2012) evaluated the sublimation rate of spherical geometry in a natural convection environment. Anderson casted specimens using paradichlorobenzene as the testing medium. The diameters used to determine the sublimation rate in this study were 4.03 cm, 6.77 cm, and 8.46 cm. He used toy tennis balls as molds to cast the specimens and placed a wood skewer into the ball before casting to be used to hang the specimen during testing. Anderson found that the paradichlorobenzene does not bond to rubber, so no release agent was required to

remove the specimen from the molds. The data acquisition was performed by the use of a Metler Toledo MS digital scale connected to a computer using LabX Direct Balance software to output mass measurements in an Excel spreadsheet every 60 seconds. The specimens were frequently observed to ensure they remained spherical throughout the tests. After the specimen became noticeably distorted and no longer spherical or after a reduction of 0.05% reduction in diameter, the tests were terminated. The data used in this research consisted of one test for each sized sphere.

The material properties and constants used for calculations are shown in below. shows the sublimation rate results along with the Sherwood, Grashof, and Rayleigh numbers calculated for each size sphere tested [5]. The calculated results yielded an equation of $Sh = 0.0113 \cdot Ra^2 + 0.9004 \cdot Ra + 11811$ correlating the data with $R^2 = 1$ [5]. Figure 3 plots the results of the Sherwood numbers and Rayleigh numbers found, giving this equation [5].

Table 5: Constants used for W. Anderson calculations.

Ambient Temperature, T_w	Gas Constant, R_v	Diffusion Coefficient, D_{AB}	ρ_v
72°F = 295.37 K	56.561 J/(kg·K)	4.13 x 10 ⁻⁰⁶ m ² /s	137 Pa
ρ_v	ρ_{air}	v_{air}	μ_{air}
8.22 x 10 ⁻⁰⁶ kg/m ³	1.22 kg/m ³	1.50x 10 ⁻⁵ m ² /s	1.84 x 10 ⁻⁵ N·s/m ²

Table 6: W. Anderson experimental results.

Diameter in m	0.0403	0.0677	0.0846
Sublimation rate kg/s	5.12 x 10 ⁻⁸	9.63 x 10 ⁻⁸	1.54 x 10 ⁻⁷
Surface area m ²	0.0051	0.014	0.022
h_m in m/s	1.22	0.81	0.83
Sherwood number	11900	13300	17100
Grashof number	19.05	90.67	176.87
Rayleigh number	69.33	329.89	643.52

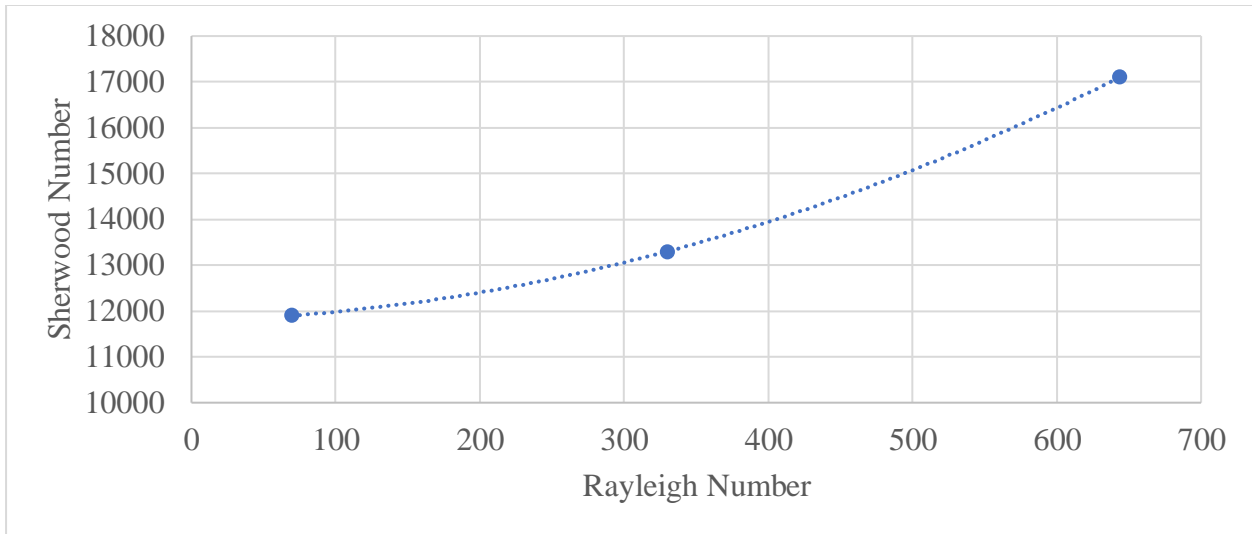


Figure 3: Plot of the Sherwood Number and Rayleigh Number for W. Anderson results.

Summary of Literature and Gaps in Knowledge

There have been many studies performed using this methodology involving multiple geometries and materials. The literature findings lack thorough research in spherical geometry. Spherical geometry has been sublimated in the past in free and forced convection environments. However, there was only one instance of research found in free convection of the spherical geometry. The data in that research only provided results for three sizes of spheres in a broad range. The results outlined in this research will fill in some of these gaps of specimen sizes not provided in that past study.

Materials and Methods

Creating Molds

In this study 99.9% pure paradichlorobenzene was used. In order to create spherical testing specimens, a mold to cast the paradichlorobenzene was needed. Paradichlorobenzene has a melting point of approximately 53°C so, to start, the mold material would be required to withstand a temperature above 70°C or so. Another goal was to keep cost down by using inexpensive materials and manufacturing processes. As for data required for this study, the goal was to collect data on four different sized spheres, this will require four different sized molds.

With all this in mind, the first plan was to design the mold in Solidworks and 3d print the mold using ABS plastic as the medium. After creating a finished mold [Figure 4], melting the paradichlorobenzene, and pouring a cast, approximately two hours were allowed for the material to cool before attempting to separate the mold. After cooling the mold could not be separated. Using a hacksaw, the mold was cut open, to discover the paradichlorobenzene had a reaction with the ABS plastic, melting the inside of the mold [Figure 5]. There were attempts creating molds using PETG and PLA plastic as well, however those plastics reacted with the paradichlorobenzene also. After these failed attempts, a decision to try molds made of silicone



Figure 1: First finished mold made from ABS plastic.



Figure 2: First casting test in ABS mold which was required to be cut open due to the paradichlorobenzene melting the plastic from a chemical reaction.

rubber was made. Some inexpensive spherical silicone baking molds were sourced online [Figure 6]. These proved to work decently and did not have any chemical reactions with the



Figure 3: Spherical silicone baking molds purchased online.

paradichlorobenzene, but the heat caused the silicone to be malleable and the molds were unable to hold the pressure of the paradichlorobenzene.

These issues could be resolved with a few design elements. What was needed was a thicker mold to take the pressure and a two-part design which self-aligned while creating a moderate mechanical lock when assembled. For this, custom silicone molds would need to be created. Solidworks was used to design mold negatives [Figure 8, Figure 9 and Figure 10] and 3d printed from ABS plastic. Each mold negative was a multi piece component featuring a removable collar, to hold the liquid silicone in place while curing, and a removable stem in the center of the top mold negative, to give a fill hole after the silicone molds were created. After printed, the mold negatives were lightly sanded, removing any small imperfections and burrs, then smoothed using a technique, involving acetone vapor, to remove the resulting textured finish and “layer lines” of 3d printing [Figure 7]. The acetone vapor bath finishing technique is



Figure 4: Pictured above, un-altered 3d printed mold negative on the left and acetone vapor smoothed mold negative on the right.

accomplished by using an electric pot with an elevated steam basket and lid. ABS plastic can be melted by acetone and acetone has a very low boiling point. Approximately half a cup of acetone is poured into the bottom of the electric pot and the object is placed in the steam basket. The lid is then placed on top of the pot and the power is turned on a very low setting. As the acetone begins to boil, a fog forming inside the pot can be seen and the part will develop a glossy sheen very quickly. As soon as the part completely glosses over turn the power off and wait 10-15 seconds before removing the lid and pulling the steam basket from the pot.

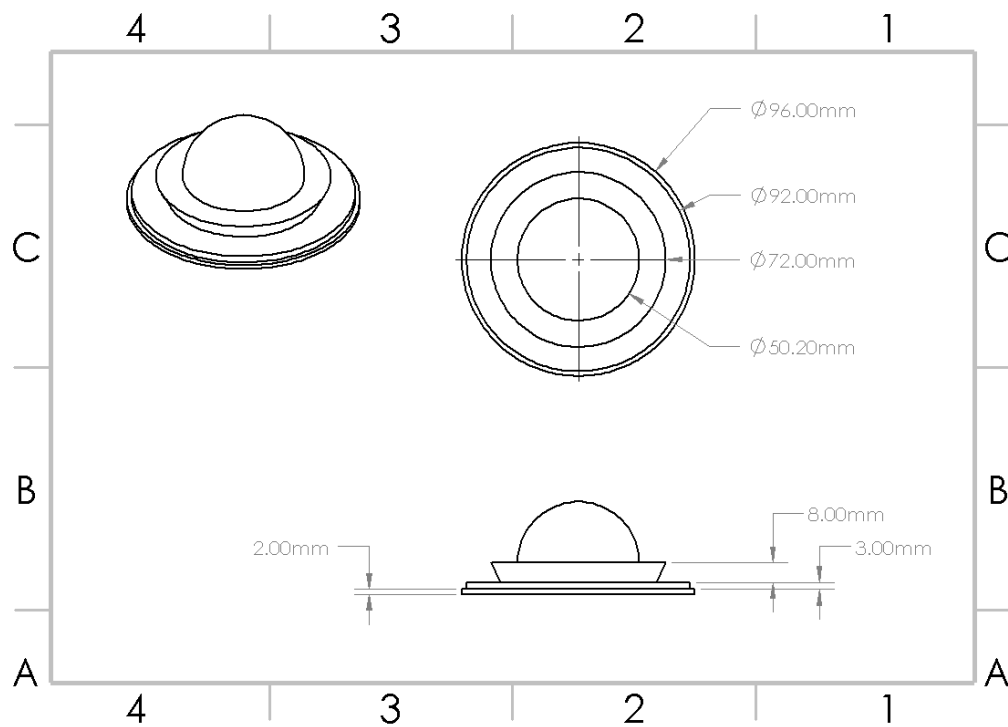


Figure 5: Technical drawing of the lower half mold negative used to create the lower silicone mold.

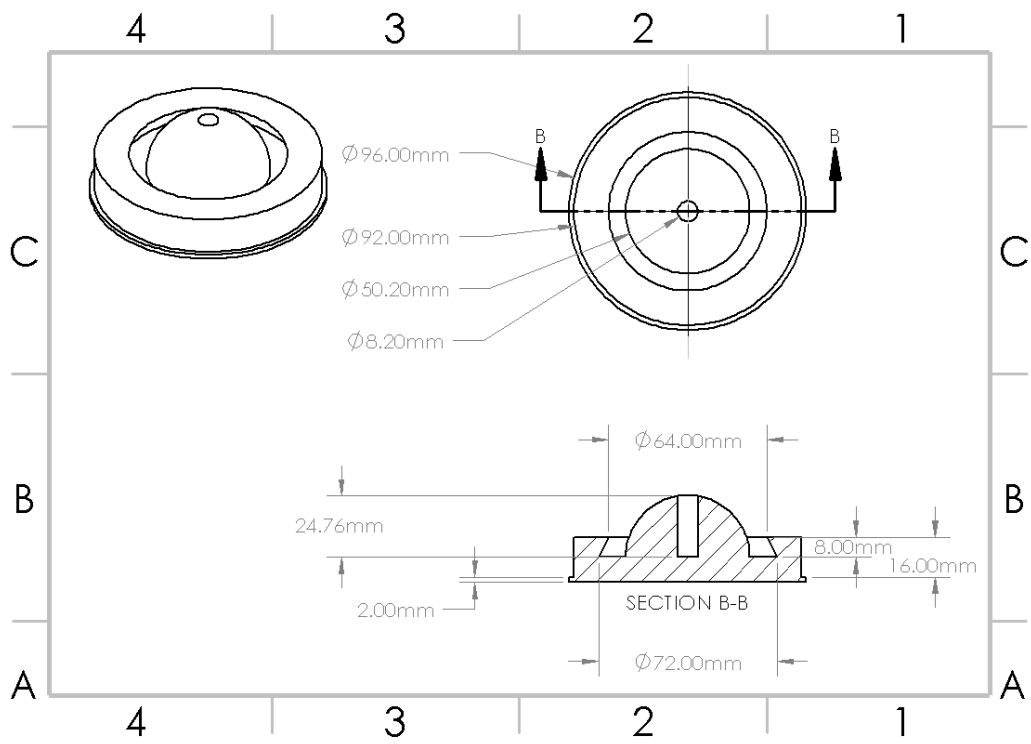


Figure 6: Technical drawing of the upper half mold negative used to create the upper silicone mold.

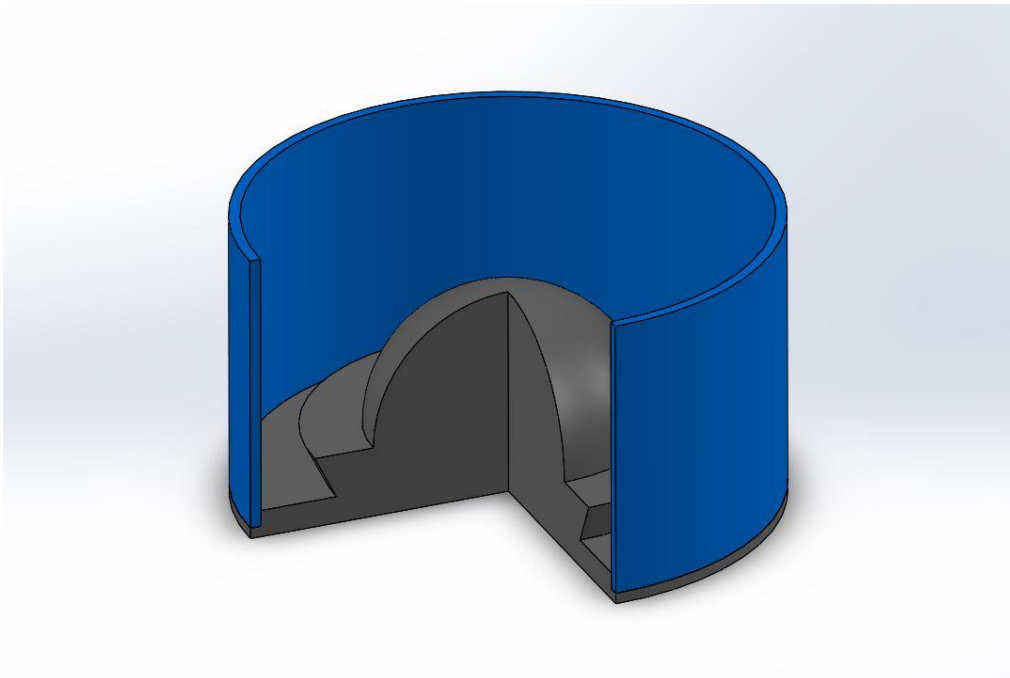


Figure 7: Cutaway view of the plastic mold negative and silicone retainer assembled.

Before assembling the mold negatives to create the silicone molds, all parts are wiped down with isopropyl alcohol. Now with the complete mold negatives assembled and ready to accept the silicone



Figure 10: Mold negatives assembled, cleaned and ready to accept silicone.

[Figure 13], the preparation for mixing the silicone can begin. The silicone mold material used, manufactured by a company named Smooth-On, is called OOMOO 30 which has a 30A shore hardness in its cured state. The silicone material is a two-part mixture, part A and part B, requiring a 1:1 mix ratio.

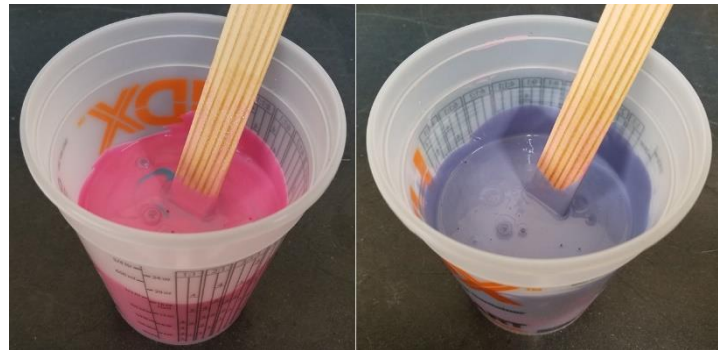


Figure 9: The silicone two-part component initially poured into mixing cup on the left and the thoroughly mixed silicone on the right.

For mixing the silicone, a generic mixing cup and paint stirrers found in the paint department at the local hardware store were used. After the silicone was thoroughly mixed, it was poured into the mold negatives [Figure



Figure 8: The silicone being poured into mold negatives.

11]. After 24 hours the mold negative was ready to be disassembled, revealing the finished mold for creating test specimens' [Figure 14, Figure 15, Figure 16, Figure 17, and Figure 18].

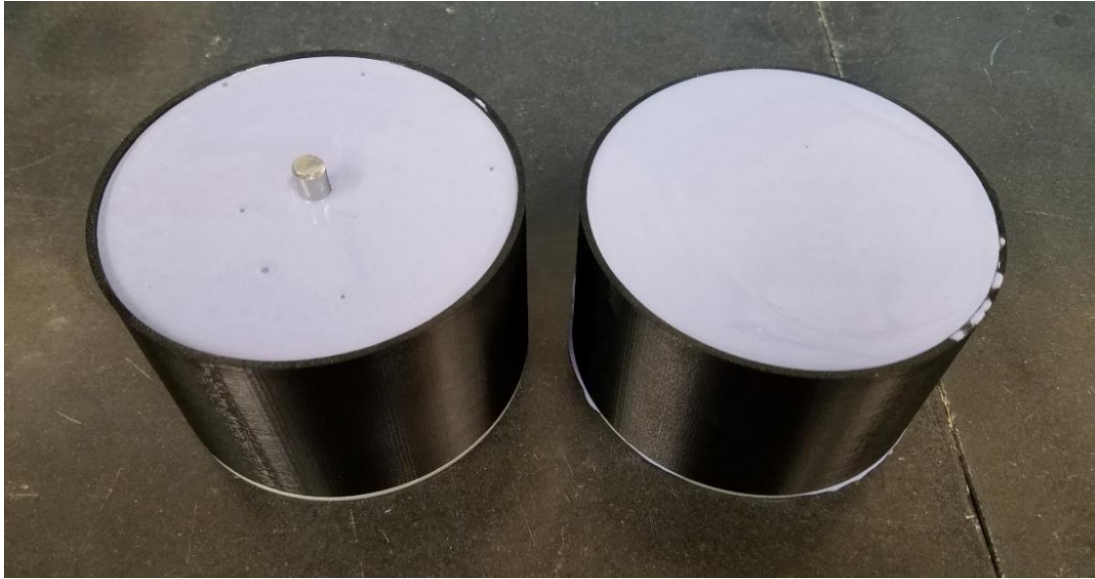


Figure 14: Silicone cured, and the mold negative is ready for disassembling.



Figure 15: Center post removed, revealing a fill hole.

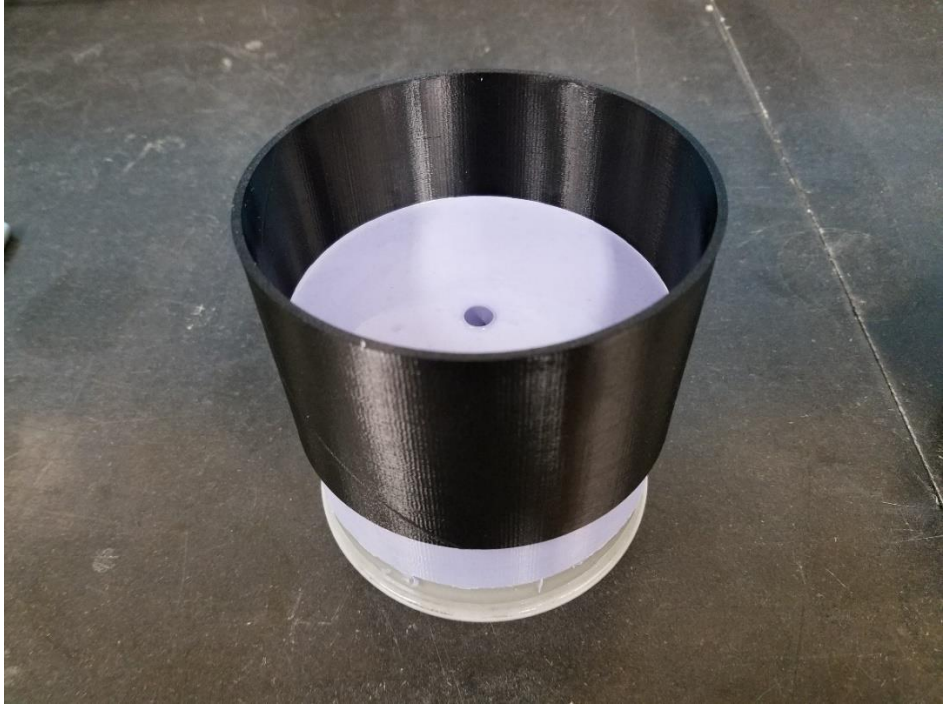


Figure 16: Removing the silicone retainer ring.



Figure 17: Silicone mold removed from mold negative.



Figure 18: All components disassembled revealing the two silicone mold halves, ready to be used.

Casting Specimens

Paradichlorobenzene has a melting point of approximately 54°C and this makes the material rather simple to melt and cast. The molds were required to be prepared before

introducing the liquid paradichlorobenzene to them and casting began. First, a way to suspend the specimen was required. For this, a piece of fishing line would be cast into each specimen. The piece of line used would be slightly melted on the tip of one end using a pocket lighter [Figure 20]. This was to prevent the line from pulling out of the



Figure 12: The tip at one end of the fishing line was melted, creating a small ball, to prevent the line from coming out of the cast specimen.

specimen after casting. Now using a sewing needle, the line could be guided through to the top of the mold, puncturing a small hole in the mold [Figure 19]. Due to the excellent elastomer

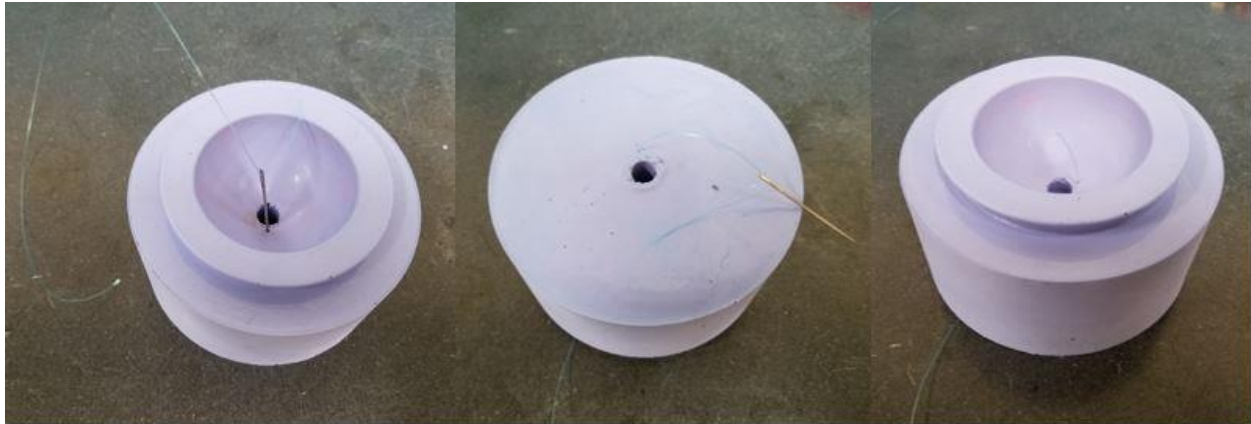


Figure 11: From left to right, the sewing needle with fishing line is fed from the inside of the mold and out through the top. The line is pulled through until the melted end of the line is even with the surface of the flange on the mold, placing the line in the center of the finished specimen.

properties of the silicone material and using a sewing needle, the resulting hole is so small it does not cause any issues with the casting procedure. Next, the inner mold surface would be cleaned with isopropyl alcohol and preheated with a heat gun. The mold was preheated to prevent flash

cooling of the liquid paradichlorobenzene which caused an undesirable rough, patchy surface on the finished casting. After this, the mold was closed and placed on a tray [Figure 21]. Paradichlorobenzene was then melted down in a small stainless-steel dish using an electric skillet [Figure 22]. The liquid paradichlorobenzene was then poured into the mold [Figure 23]. This process was repeated until the mold was full. The mold was then placed in a small refrigerator, decreasing the time taken to solidify. The mold would stay in the refrigerator for 30 minutes to one hour, depending on the size of the specimen, then removed. The mold would then be topped off and allowed to solidify in ambient conditions. It was observed the paradichlorobenzene would contract when cooling and the evaporation rate when heated was high, lowering the yield of return from melting the raw pellets. The tray was used to prevent the mold from deforming while being transported to and from the refrigerator. The tray is made from 3003 aluminum, which has a high thermal conductivity, and to allow the mold to cool as evenly as possible, a piece of thermal insulator was used between the tray and mold.



Figure 13: Assembled mold placed on transportation tray with thermal insulation pad.



Figure 14: Melting paradichlorobenzene moth balls in stainless-steel dish on electric skillet.



Figure 15: Pouring melted paradichlorobenzene into silicone mold.

After the specimen had been allowed to cool, the mold was ready to separate. When separating the mold, removing the lower half from the upper half is performed first (Figure 25). With the specimen remaining in the upper half, it can be pulled straight out (Figure 25). The plug



Figure 17: Mold separated, specimen removed, then trimmed fill plug excess, and tied a loop in the string for suspending.

of material left behind from the fill hole and mold seam flashing can easily be trimmed with a razor knife (Figure 25). A loop could then be tied in the string cast into the specimen for hanging



Figure 16: Specimen hung on the weigh below hook and ready for starting mass data acquisition.

purposes (Figure 25). At this point the specimen was ready to be hung on the scale to begin testing (Figure 24).

Data Acquisition

The first requirement for collecting data was to determine what data would be useful in this research. For the equations used in this study, diameter, mass loss over time, and testing environment temperature were required. The scale used was a Mettler Toledo PB153-S, which records to the nearest thousandth of a gram with an uncertainty of $\pm 0.012\%$. The scale was calibrated prior to collecting data. A visual basic code was written in Microsoft Excel to record the mass every 5 minutes from the scale to a spreadsheet. As for the testing environment temperature, a DHT-22 sensor was used connected to an Arduino Nano. An Arduino code was written to record temperature and humidity every 5 minutes to an onboard SD card. The diameter was measured at the beginning and end of testing using a pair of digital calipers.

A trial and error period was performed, beginning testing, to determine the best testing environment and equipment configuration. The scale used was equipped with a draft shield enclosure and in the initial trials the enclosure remained on the scale with all shielding doors left in the open position, two side doors and one overhead, during testing allowing the paradichlorobenzene vapor to escape. This proved to negatively affect the specimens, for they slowly became pill shaped as they sublimated. This displayed the sublimation was not occurring evenly over the surface. After this, a scale stand that allowed for a weigh below configuration was designed and built. This design places the test specimen away from any objects that may interfere with the sublimation process and proved to be successful. The testing environment was carefully chosen as well and for this, a large and low traffic room was desired. A room that is 55x43x18 cubic feet and adequately ventilated was used, which is large enough to prevent the testing atmosphere from getting saturated with paradichlorobenzene vapors, slowing the sublimation rate.

After specimens were cast, trimmed, and ready for testing, the first data recorded was the diameter. The diameter was recorded using a pair of digital calipers, taking seven measurements, to verify spherical geometry. Each trial collected mass and temperature data for 24-48 hours, depending on size, to verify the mass transfer rate was consistent and no anomalies occurred during testing. When the trial was terminated, the diameter was measured again to verify the specimen sublimated evenly across the surface. After finalizing the testing environment and methods, a total of three trials were performed for each sized sphere.

There were test trials performed to monitor the reduction in diameter during sublimation. This data was used to determine the amount of time for each sized specimen to reach a 1% reduction in diameter. Each trial was run for 24-48 hours, however only the time taken to have a diameter reduction of 1% was used for the results. A total of 65 trials were performed throughout testing to get the most accurate results possible. Of these trials, three of each sized specimen were chosen to be used for the results. There were many trials where complications occurred causing faulty data showing fluctuations in the sublimation rate when plotted. The complications were issues in the testing environment, such as the room HVAC running too fast for long periods of time, or the specimen sublimating down to reveal an air pocket in the casting, altering the mass transfer rate.

Equations

To find the Sherwood number, the overall mass transfer coefficient was required. There are two mass transfer equations used here to obtain this value, Fick's Law and the molar flux equation. These equations describe molar flux using vapor concentration differences which cause density gradients in mass transfer. Fick's Law in mass transfer is analogous to Fourier's Law in heat transfer and the molar flux equation is analogous to Newton's Law of Cooling.

Fick's Law:

$$N_A = -D_{AB} \frac{\partial C_A}{\partial r} \Big|_r \quad (1)$$

Molar Flux:

$$N_A = h_m (C_A - C_\infty) \quad (2)$$

N_A is defined as the rate of mass flow per unit area so substituting N_A for $\frac{\dot{m}}{A_s}$ in eq (2) yields:

$$h_m = \frac{\dot{m}}{A_s(\rho_{v,s} - \rho_{v,\infty})} \quad (3)$$

The vapor density very far from the surface of the sphere can be assumed to be zero. This can be assumed due to the testing taking place in a 42,000 cu. ft. facility with adequate ventilation.

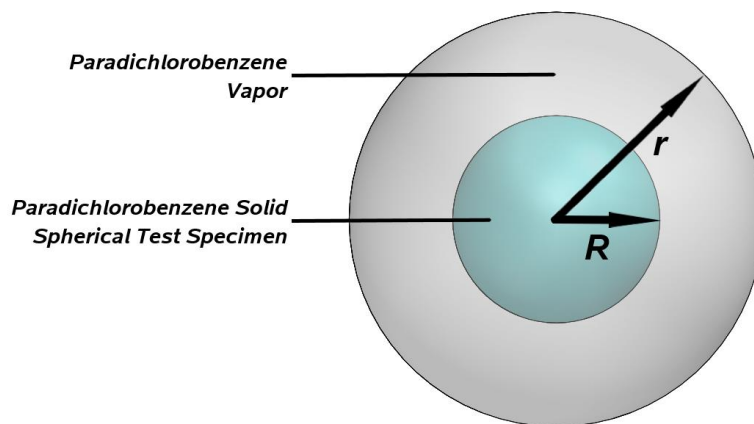


Figure 26: When $r=R$ the vapor density is equal to C_A . At a far distance, as $r \rightarrow \infty$, $C_\infty = 0$.

The vapor density at the surface is assumed to behave as an ideal gas, therefore can be calculated using the ideal gas law. For this, the vapor pressure and gas constant must be acquired. The vapor pressure, for paradichlorobenzene, can be calculated using an empirical equation developed by Sogin [7]:

$$P_{v,s} = 10^{\left(B_1 - \frac{B_2}{T_s}\right)} = 10^{\left(11.518 - \frac{5946}{T_s}\right)} \quad (4)$$

B_1 and B_2 are material constants while T_s is the specimen temperature at its surface in degrees Rankine and the pressure is given in psi. The gas constant, R , used here is what Sogin [7] used in his research. With these values the vapor density can be determined using the ideal gas law:

$$\rho_{v,s} = \frac{P_{v,s}}{R_v T_s} \quad (5)$$

The sublimation rate, \dot{m} , was found experimentally and the diffusion coefficient, D_{AB} , used was experimentally found by Sogin [7].

These values along with the experimental data acquired can now be used to find the Grashof, Schmidt, Raleigh, and Sherwood number, all dimensionless numbers, to correlate the data. The Sherwood number, analogous to the Nusselt number in heat transfer, represents the ratio of the convective mass transfer to the rate of diffusive mass transfer. The Grashof number approximates the ratio of the buoyancy to viscous force acting on a fluid. The Schmidt number, analogous to the Prandtl number in heat transfer, is defined as the ratio of kinematic viscosity, or momentum diffusivity, to mass diffusivity. The Rayleigh number is the product of the Grashof and Schmidt number.

$$Sh = \frac{h_m D}{D_{AB}} \quad (6)$$

$$Gr = \frac{\rho_{air} D^3 g (\rho_{v,s} - \rho_{v,\infty})}{\mu^2} \quad (7)$$

$$Sc = \frac{\nu}{D_{AB}} \quad (8)$$

$$Ra = Gr \cdot Sc = \frac{\rho_{air} D^3 g (\rho_{v,s} - \rho_{v,\infty})}{\mu^2} \cdot \frac{\nu}{D_{AB}} \quad (9)$$

Results

The constants required for calculations were found and shown below. The mass loss over time data was collected and plotted, for the four different sized spheres, in individual spreadsheets with the mass of the sphere on the vertical axis and the time on the horizontal axis. In each result the mass loss over time was not perfectly linear over the testing duration and the decrease in sublimation rate as time progressed could be seen in the plots.

Table 7: Constants used for calculations.

Ambient Temperature, T_w	72°F = 22.22°C = 295.4 K	
Gas Constant, R_v	56.55 J/kg·K	[7]
Diffusion Coefficient, D_{AB}	4.13E -06 m ² /s	[7]
Kinematic Viscosity, ν_{air}	1.53E -05 m ² /s	[8]
Schmidt number, Sc	3.69	
Absolute Viscosity, μ_{air}	1.27E -05 N·s/m ²	[8]
Density of Air, ρ_{air}	1.197 kg/m ³	[8]
Partial Pressure of Paradichlorobenzene Vapor, P_v	93.8 Pa	(4)
Density of Paradichlorobenzene, ρ_v	0.005616 kg/m ³	(5)
Gravity, g	9.81 m/s ²	

Using the mass transfer results along with the constants above, the Sherwood number and Rayleigh number could be plotted against each other. Goldstein et al. notes, to minimize the separate dependence of the Sherwood number on the Schmidt number, the Rayleigh number should be used instead of the Grashof number for mass transfer correlations [9]. Tables 8-11 below provide these results and Figures 26-37 in the appendix show the mass transfer rates plotted.

Table 8: Reduced data for 30mm sphere trials.

30mm Sphere			
	Trial 1	Trial 2	Trial 3
\dot{m} (kg/s)	3.90E-08	3.87E-08	3.85E-08
Diameter (m)	0.03063	0.03061	0.03051
Radius (m)	0.01532	0.01531	0.01526
Area (m²)	0.002947	0.002944	0.002924
h_m (m/s)	0.002355	0.002340	0.002347
Sh	17.46	17.34	17.34
Gr	11660	11637	11524
Ra	43084	43000	42580

Table 9: Reduced data for 40mm sphere trials.

40mm Sphere			
	Trial 4	Trial 5	Trial 6
\dot{m} (kg/s)	5.65E-08	5.59E-08	5.69E-08
Diameter (m)	0.04052	0.04054	0.04060
Radius (m)	0.02026	0.02027	0.02030
Area (m²)	0.005158	0.005163	0.005178
h_m (m/s)	0.001951	0.001927	0.001956
Sh	19.14	18.92	19.23
Gr	26995	27035	27155
Ra	99743	99891	100335

Table 10: Reduced data for 50mm sphere trials.

50mm Sphere			
	Trial 7	Trial 8	Trial 9
\dot{m} (kg/s)	7.85E-08	7.86E-08	7.92E-08
Diameter (m)	0.05005	0.05003	0.05014
Radius (m)	0.02503	0.02502	0.02507
Area (m²)	0.007870	0.007863	0.007898
h_m (m/s)	0.001777	0.001779	0.001786
Sh	21.53	21.55	21.68
Gr	50872	50811	51147
Ra	187969	187744	188985

Table 11: Reduced data for 58mm sphere trials.

58mm Sphere			
	Trial 10	Trial 11	Trial 12
\dot{m} (kg/s)	1.06E-07	1.06E-07	1.05E-07
Diameter (m)	0.05846	0.05842	0.05837
Radius (m)	0.02923	0.02921	0.02919
Area (m²)	0.010737	0.010722	0.010704
h_m (m/s)	0.001752	0.001762	0.001755
Sh	24.80	24.93	24.80
Gr	81067	80901	80694
Ra	299537	298923	298156

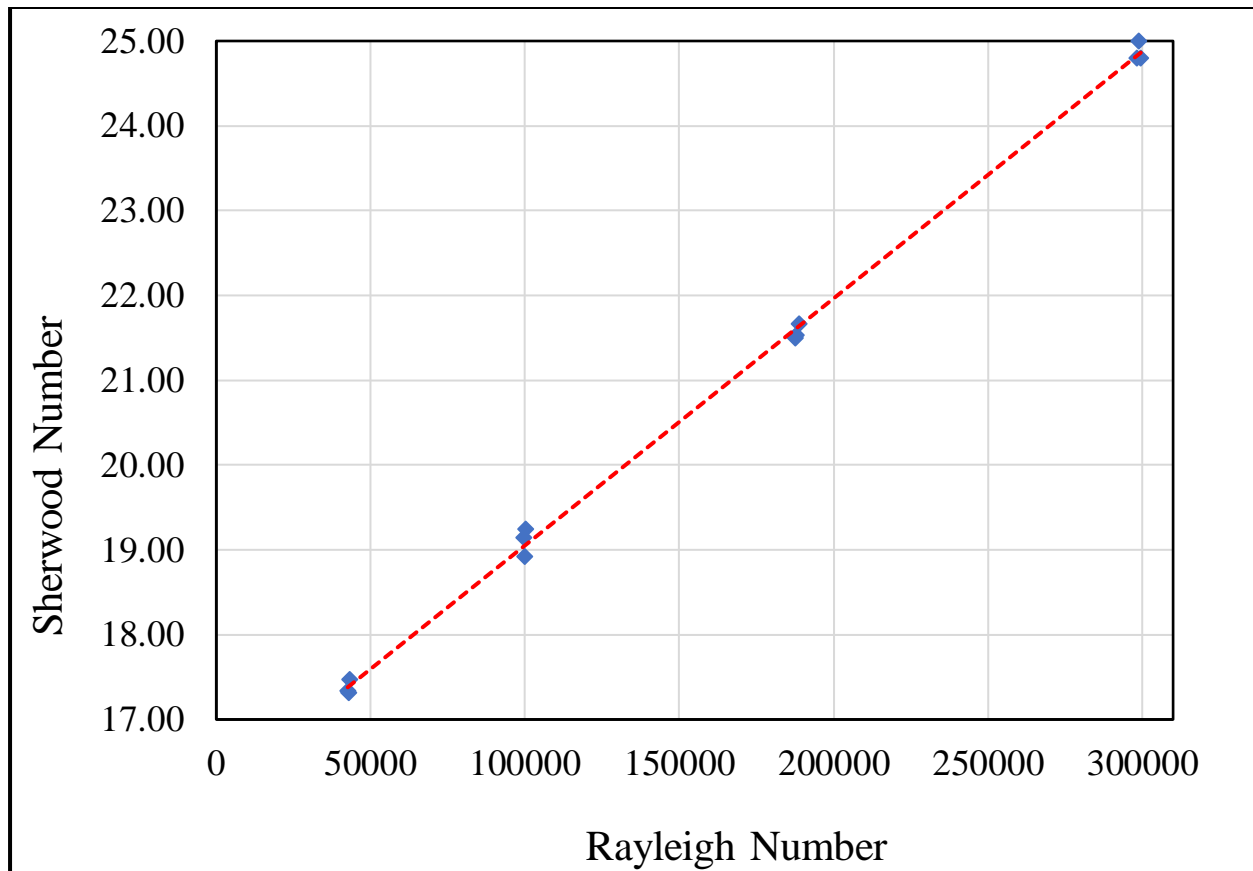


Figure 27: Reduced data results plotting Sherwood number versus Rayleigh number.

The results yielded an equation describing the Sherwood number as

$$Sh = 2.91 \times 10^{-5} \cdot Ra + 16.1 \text{ with an } R^2 \text{ value of } 0.999.$$

Overall Conclusion

Discussion and Conclusion

The trials were terminated after the specimen's diameter had been reduced by 1%. The data collection results were plotted to obtain the mass transfer rate. These results were used to calculate the Sherwood and Raleigh number and get a correlation between these two numbers. With the Sherwood and Rayleigh numbers plotted a linear slope was found.

Various specimens were allowed to continue sublimating after the trials were complete during this study. No data was collected during this extension, however this allowed further observation on how the geometry of the specimen changed over an extended amount of time. These observation specimens were left alone to sublimate for 1-4 weeks. The specimens would eventually become pear shaped after several days. This change in geometry is believed to be due to the boundary layer of the paradichlorobenzene vapor. The specimens would remain smooth and glassy, [8]but many pits would form on the surface due to buried air pockets in the casting.

There were fluctuations in several graphs which could have been caused by several factors. Occasionally the lab would have been used by numerous people causing turbulent air. Also, the specimens would sometimes experience strong drafts due to obscure HVAC operations in the lab. There were occasions where the specimens had casting defects such as large air pockets just below the surface and diameter inconsistencies or being out of round. The air pockets were subject to the paradichlorobenzene contracting as it cooled and solidified. These air pockets also caused each specimen of the same size to fluctuate in mass. The molds are two part and made from silicone rubber, so therefore are flexible, and with this the casting can suffer from minor inconsistencies. The smaller the test specimen was, the more sensitive the data was so

there was much less room for error. It was also observed in the later experiments after melting down the paradichlorobenzene and casting the same material repeatedly was causing the leftover material in the stainless-steel dish to solidify differently. When fresh material was melted down and allowed to solidify, the entire surface developed small to medium sized crystals and remained very clear. After recycling the material from previous castings two or three times over, the leftover material that solidified in the dish no longer formed crystals and went from clear in the heated, liquid form to white and very cloudy in the cooled, solid form. It was not verified if this caused any error in experimentation and if this was due to reheating or impurities from the environment.

Recommendation for Future Work

A few recommendations to expand on this research would be using different sublimating materials, testing larger sized spheres, and testing other geometries. It would be interesting to see the same dimension specimens tested cast from naphthalene. These results could be compared and possibly find any sources of errors. Also, the sphere sizes from this research were limited by the equipment which was accessible. The balance used in this research only supported enough mass for a 58mm sphere. The data collection from the small sizes in this research are easily tarnished by such minor influences making the margin for error very small. It would be recommended to test much larger spheres, adding data and results to correlate the results from this research. Another recommendation would be to test other geometries other than spheres. In the past plates and cylinders have been studied. A more complex geometry could be experimented with such as a fin array. Lastly, forced convection could be studied. This could be done using the facilities available open loop wind tunnel. Finding a suitable testing environment proved to be the most challenging part of this research due to the sensitivity of the mass transfer

rate to such small drafts. The wind tunnel is very consistent with the power input to flow rate ratio.

References

- [1] W. G. Mathers, J. A J Madden and E. L. Piret, "Simultaneous Heat and Mass Transfer in Free Convection," *Industrial & Engineering Chemistry*, vol. 49, no. 6, pp. 1025-1035, 1957.
- [2] S. Krishnan. [Online]. Available:
<https://people.clarkson.edu/~skrishna/CH351%20Mass%20Transfer%2021Sep07.pdf>.
- [3] R. R. Schmidt, "Use of Napthalene Sublimation Technique for Obtaining Accurate Heat Transfer Coefficients in Electronic Cooling Applications," *Electronics Cooling*, 2001.
- [4] K. Bautista, "Sublimating Paradichlorobenzene Cylinders Oriented Horizontally in a Natural Convection Environment," *Heat and Mass Transfer*, vol. 1, no. 1, 2017.
- [5] W. B. a. J. W. S. Snapp, "Sublimation of Vertically Oriented Paradichlorobenzene Cylinders in a Natural Convection Environment," *Heat and Mass Transfer*, vol. 48, no. 6, pp. 1005-1010, 2011.
- [6] L. W. a. J. W. S. Fite, "Mass Transfer from a Sublimating Napthalene Cylinder to a Crossflow of Air," *Applied Energy*, vol. 38, no. 1, pp. 21-32, 1991.
- [7] H. H. Sogin, "Sublimation From Disks to Air Streams Flowing Normal to Their Surfaces," *Transactions of the American Society of Mechanical Engineers*, vol. 80, pp. 61-69, 1958.
- [8] W. S. Janna, *Engineering Heat Transfer*, New York: CRC Press, 2000.
- [9] R. Goldstein, E. Sparrow and D. Jones, "Natural Convection Mass Transfer Adjacent to Horizontal Plates," *International Journal of Heat and Mass Transfer*, vol. 16, no. 5, pp. 1025-1035, 1973.

Appendix

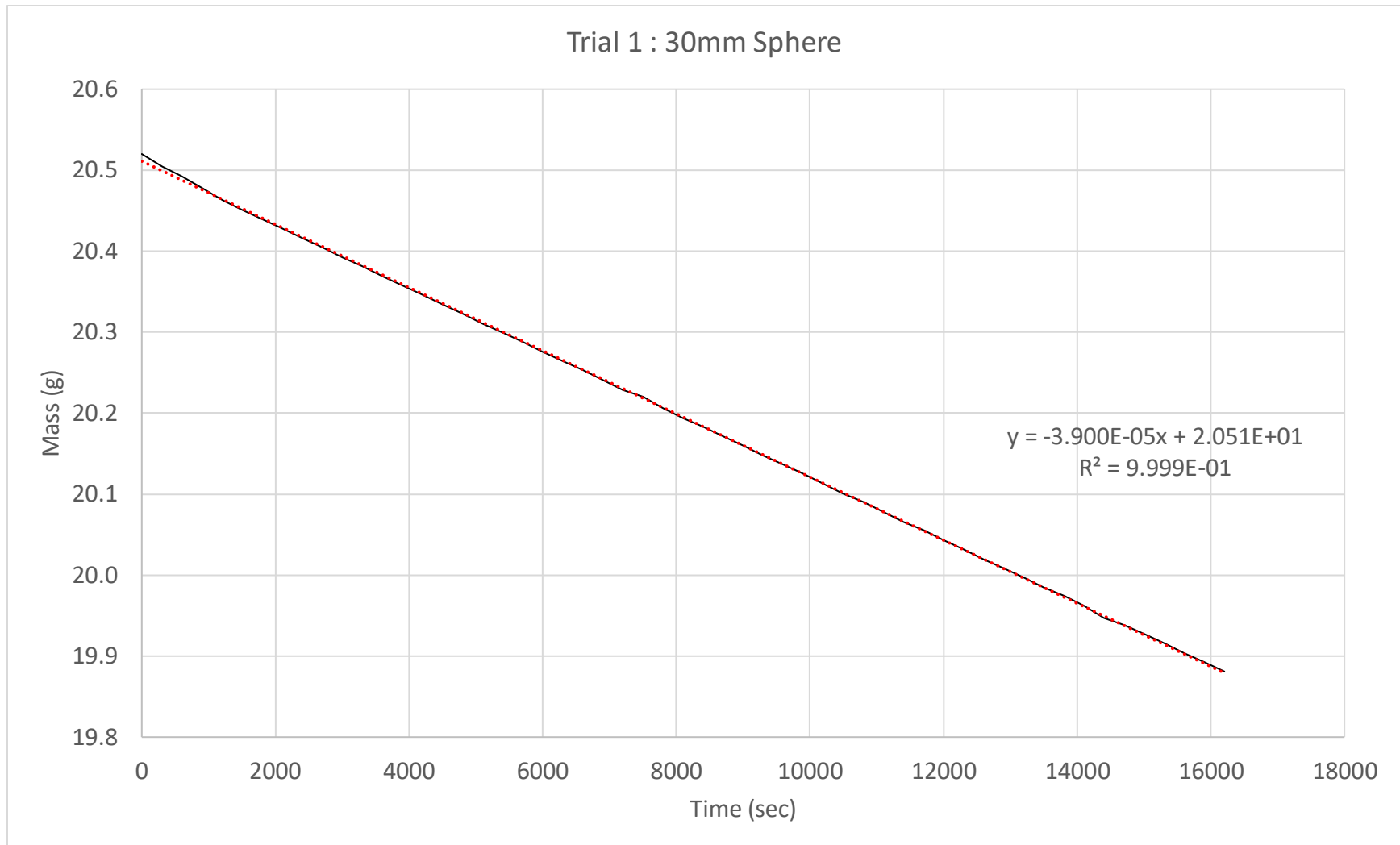


Figure 28: Experimental mass transfer rate plotted for trial 1.

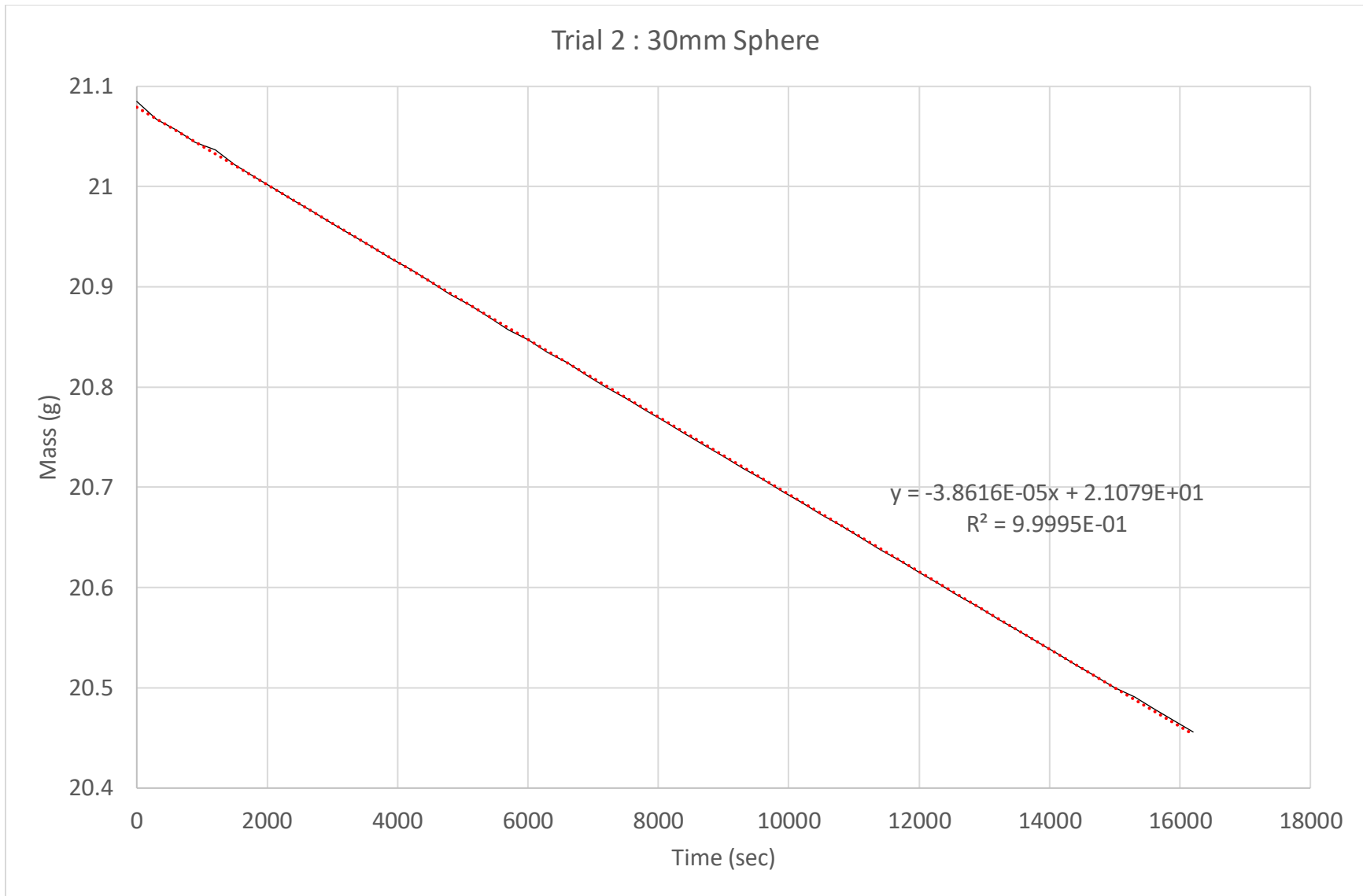


Figure 29: Experimental mass transfer rate plotted for trial 2.

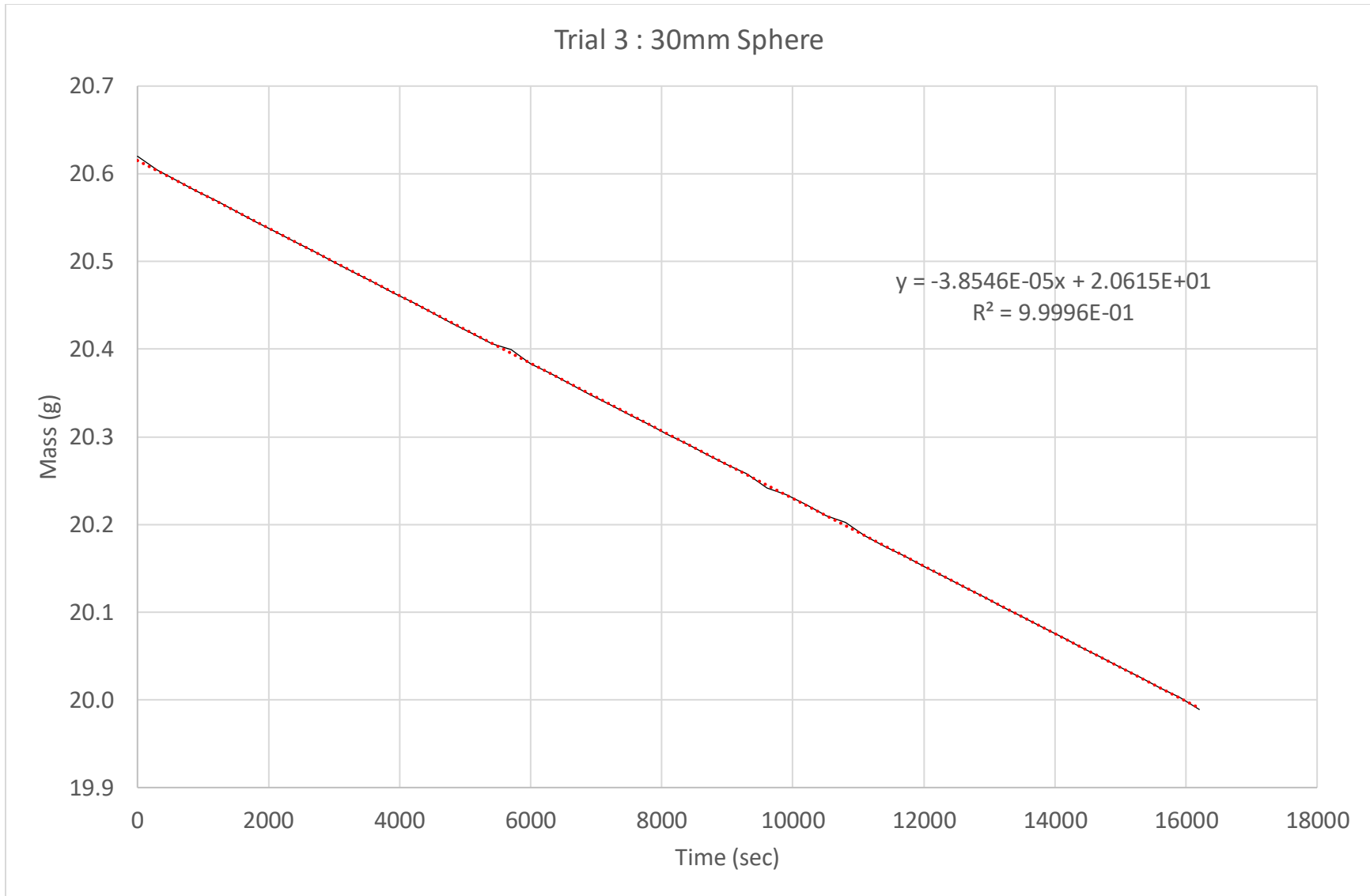


Figure 30: Experimental mass transfer rate plotted for trial 3.

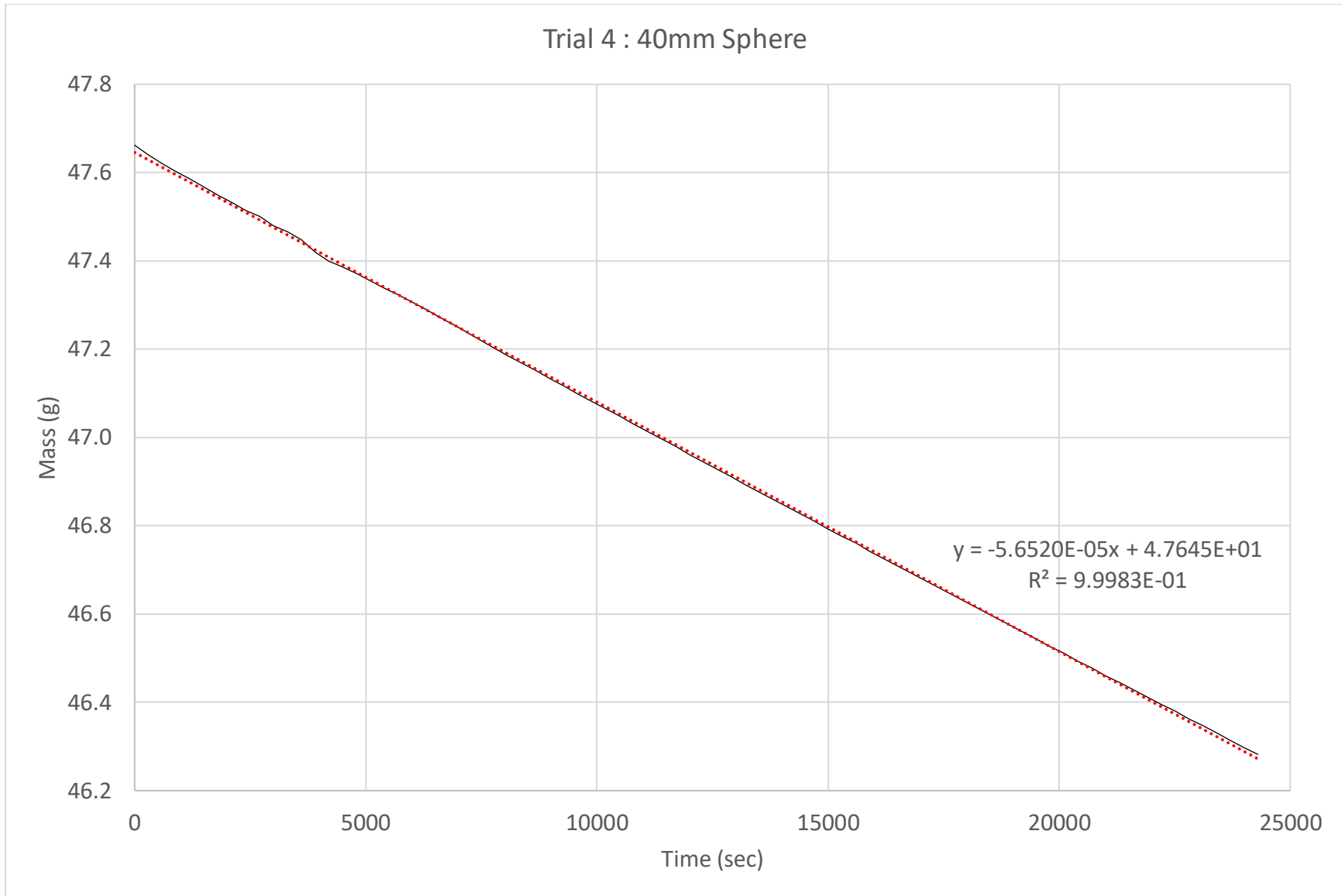


Figure 31: Experimental mass transfer rate plotted for trial 4.

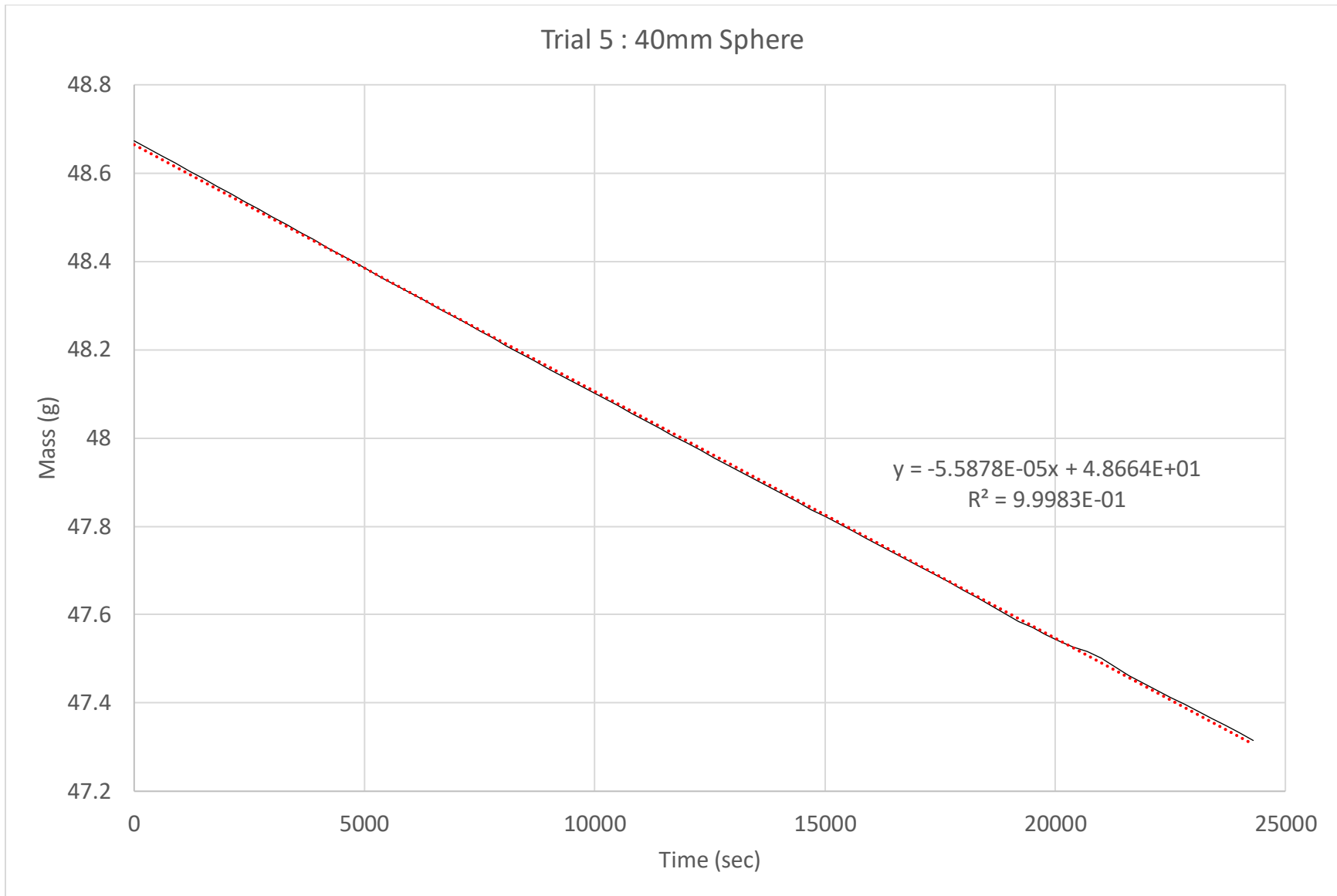


Figure 32: Experimental mass transfer rate plotted for trial 5.

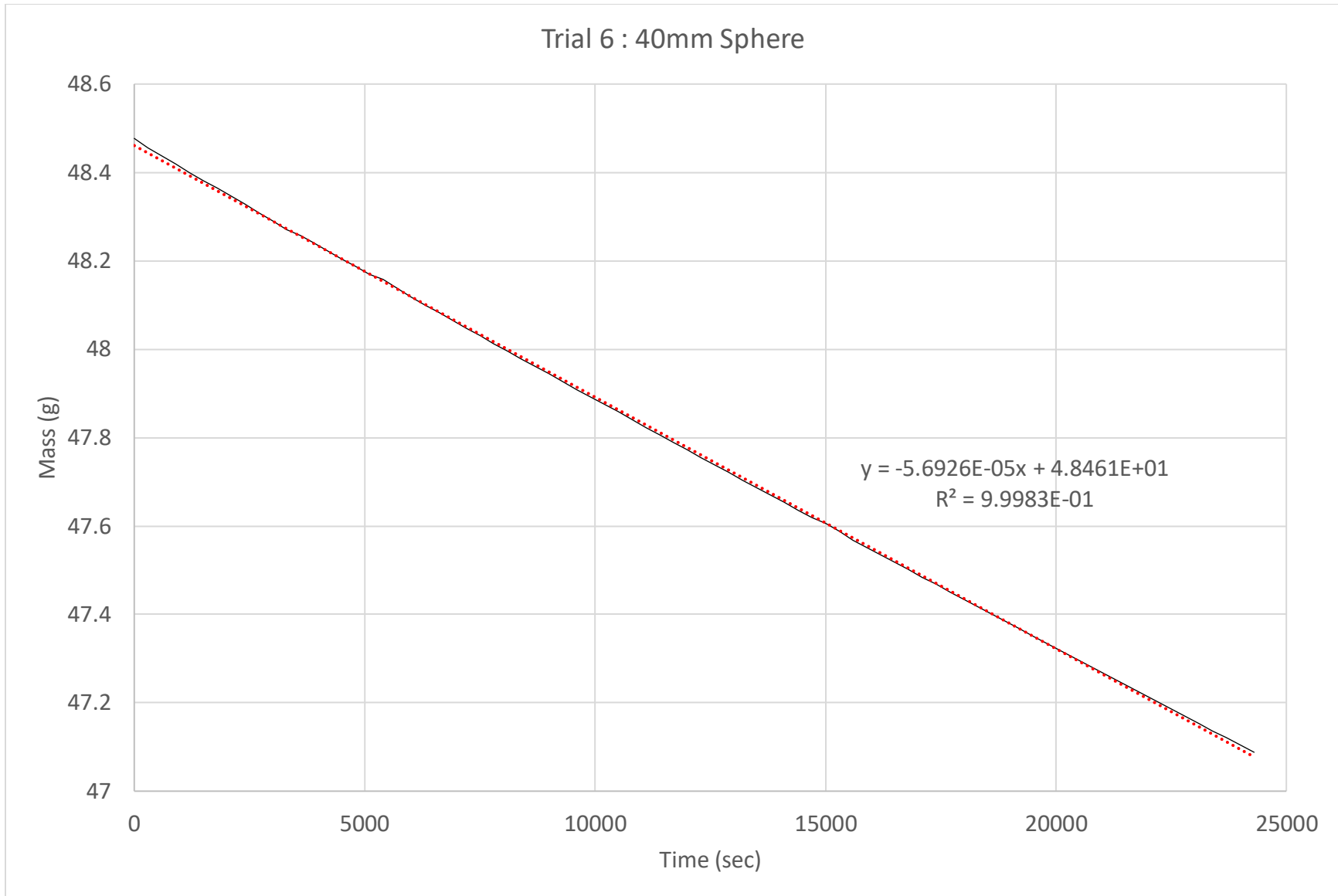


Figure 33: Experimental mass transfer rate plotted for trial 6.

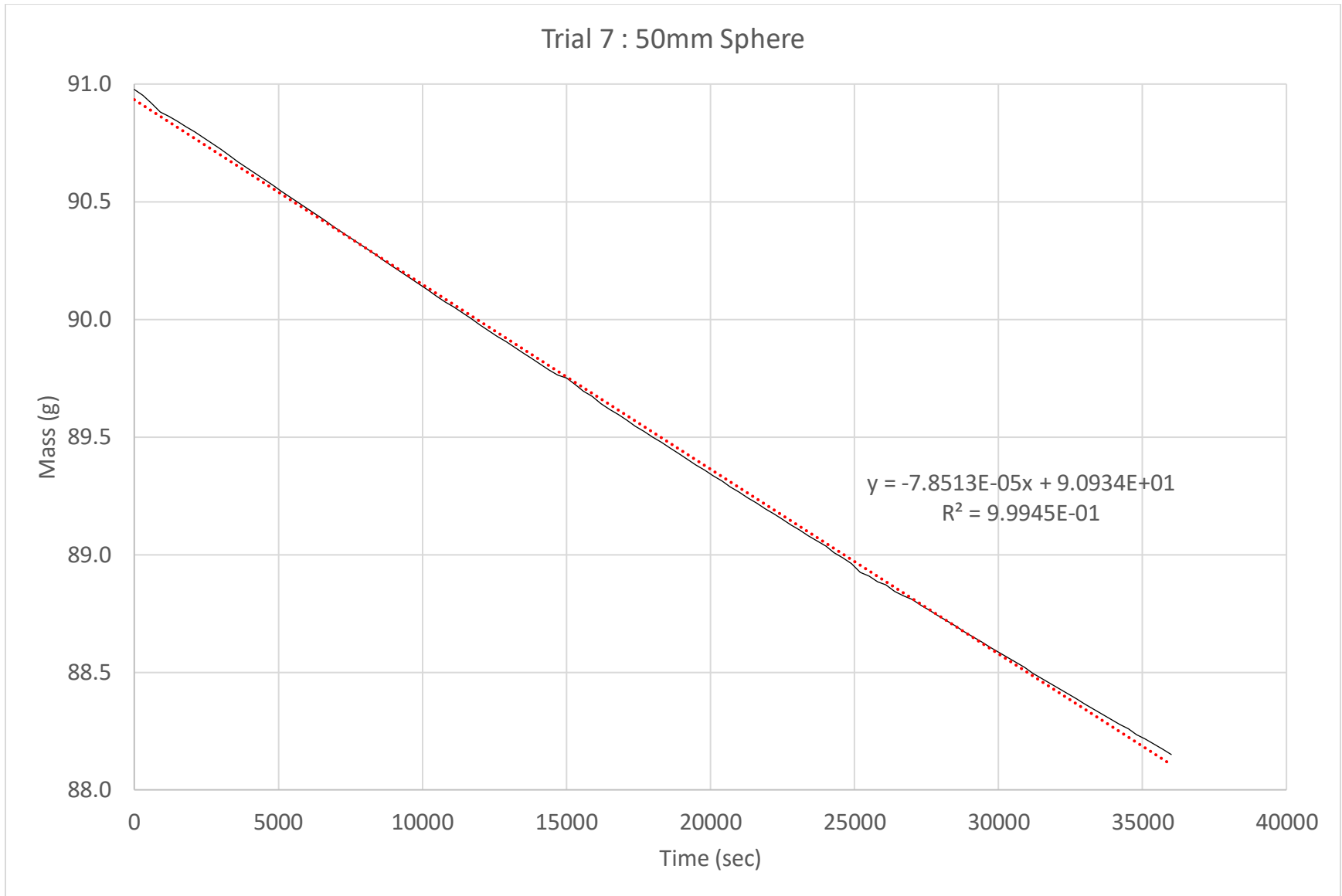


Figure 34: Experimental mass transfer rate plotted for trial 7.

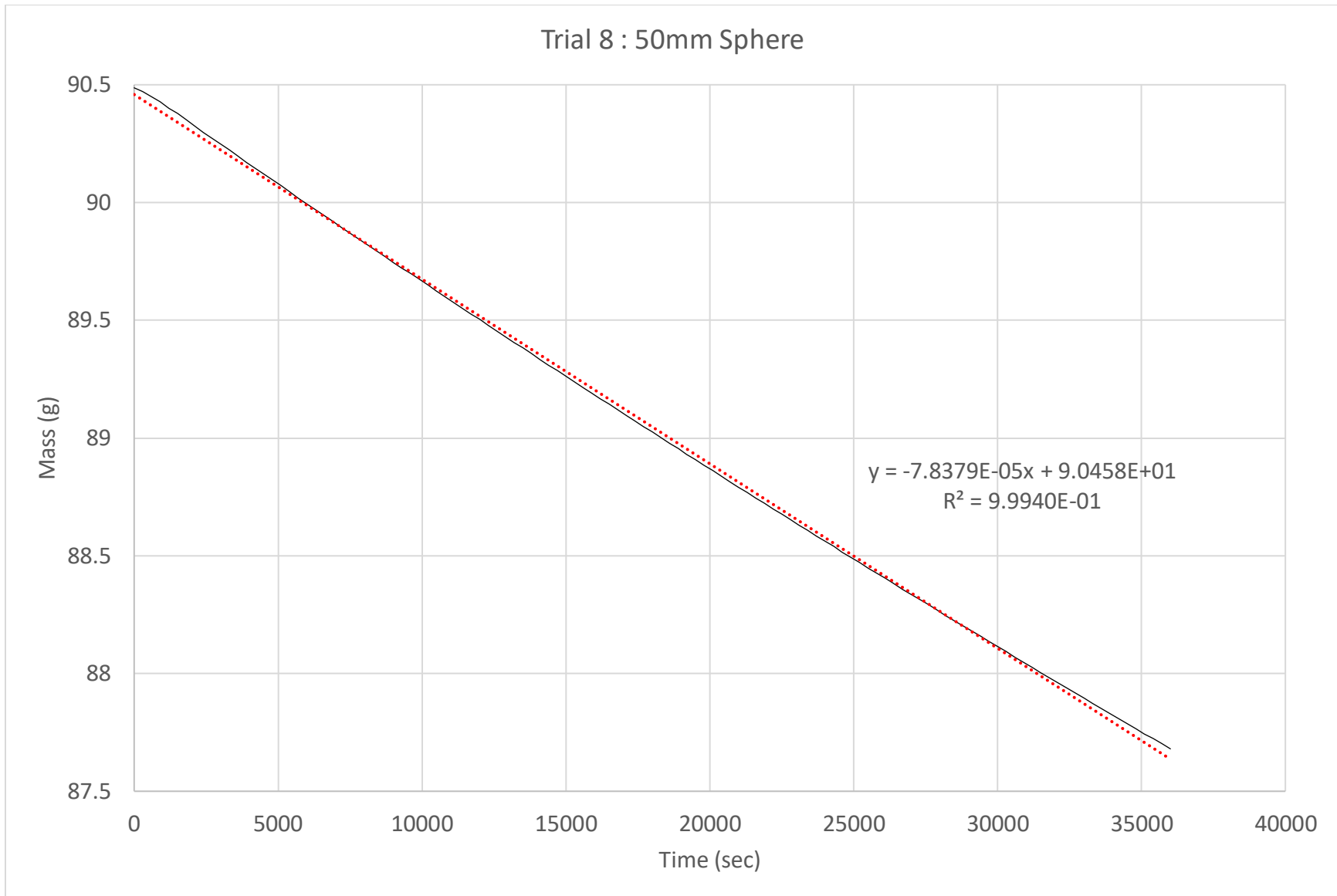


Figure 35: Experimental mass transfer rate plotted for trial 8.

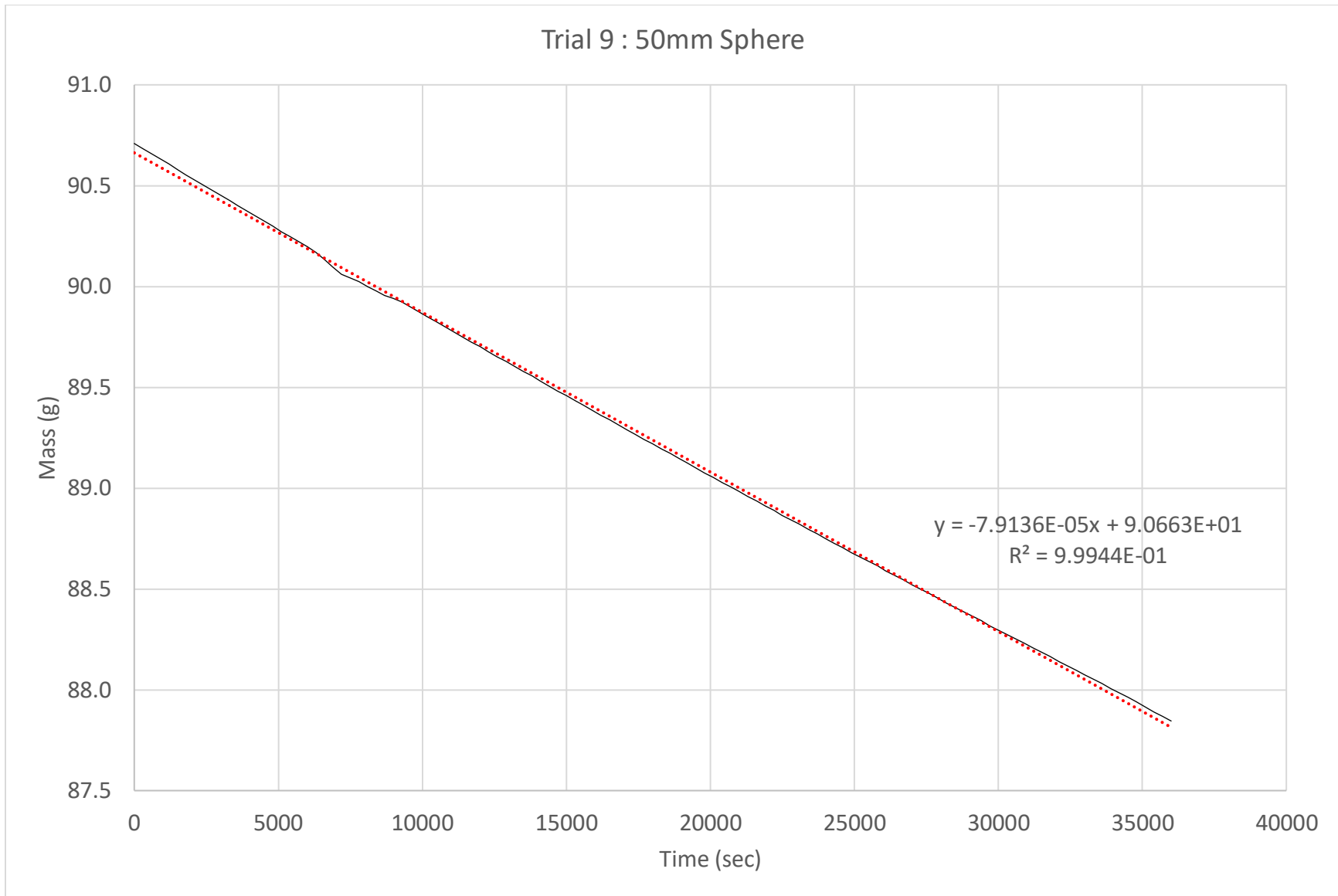


Figure 36: Experimental mass transfer rate plotted for trial 9.

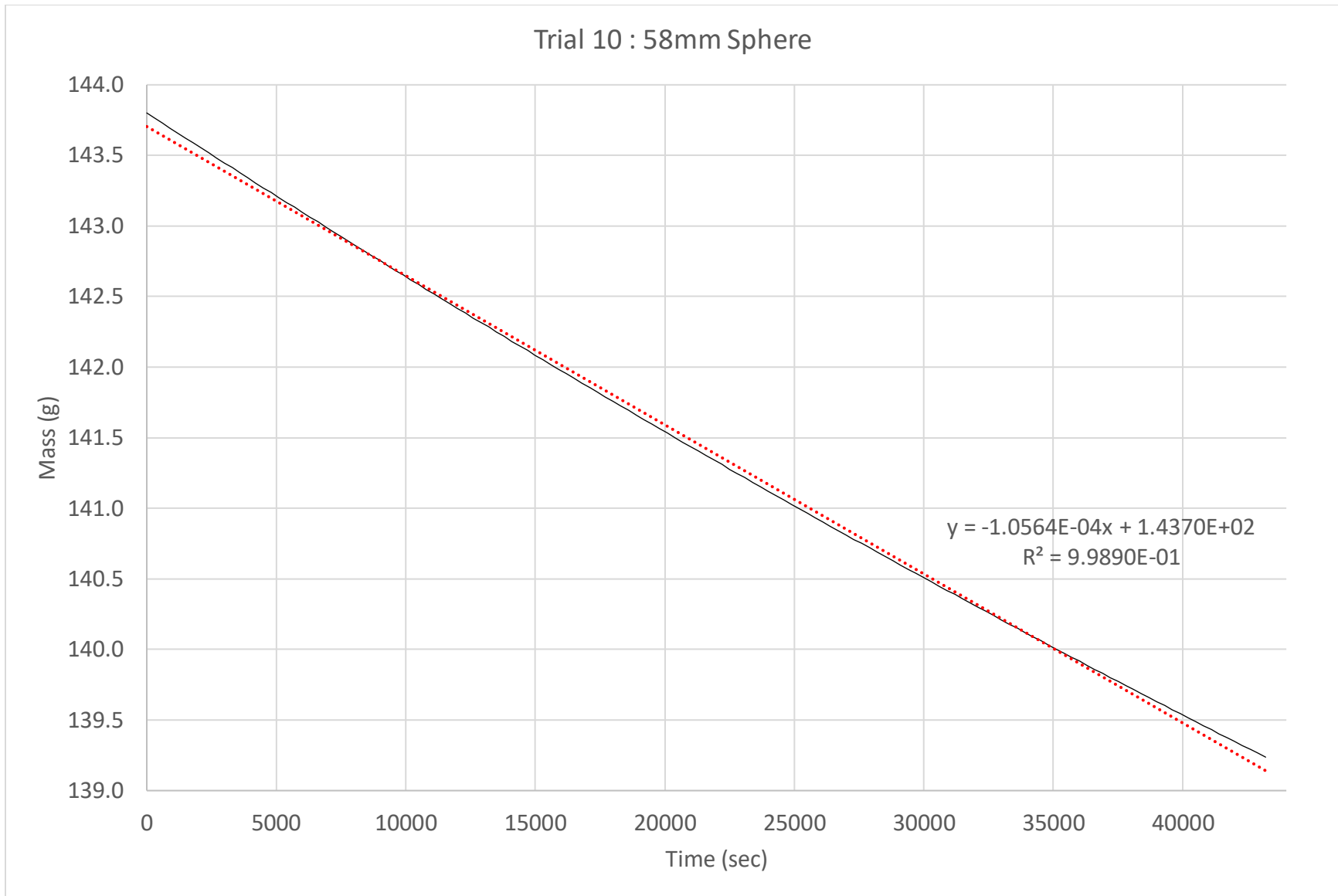


Figure 37: Experimental mass transfer rate plotted for trial 10.

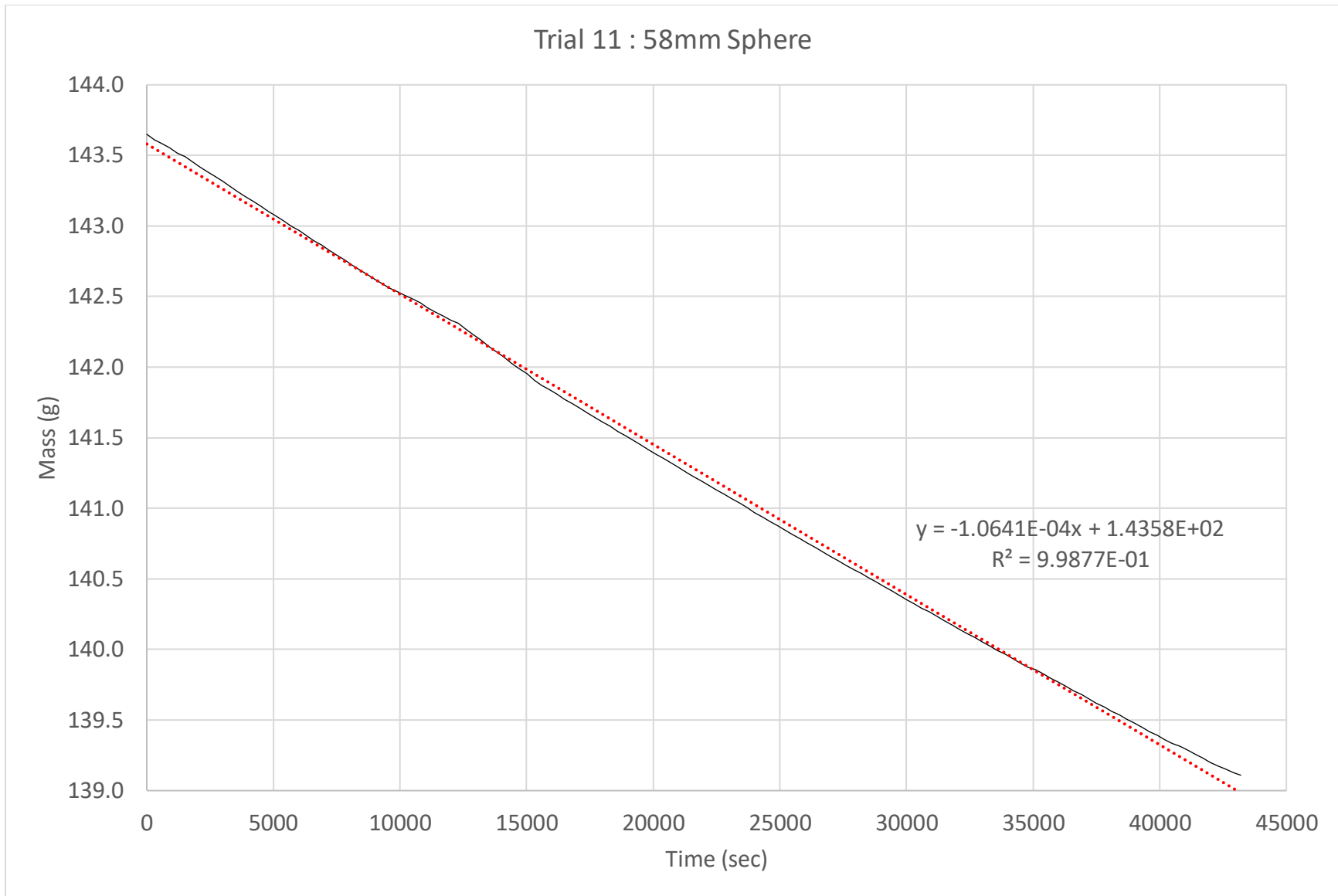


Figure 38: Experimental mass transfer rate plotted for trial 11.

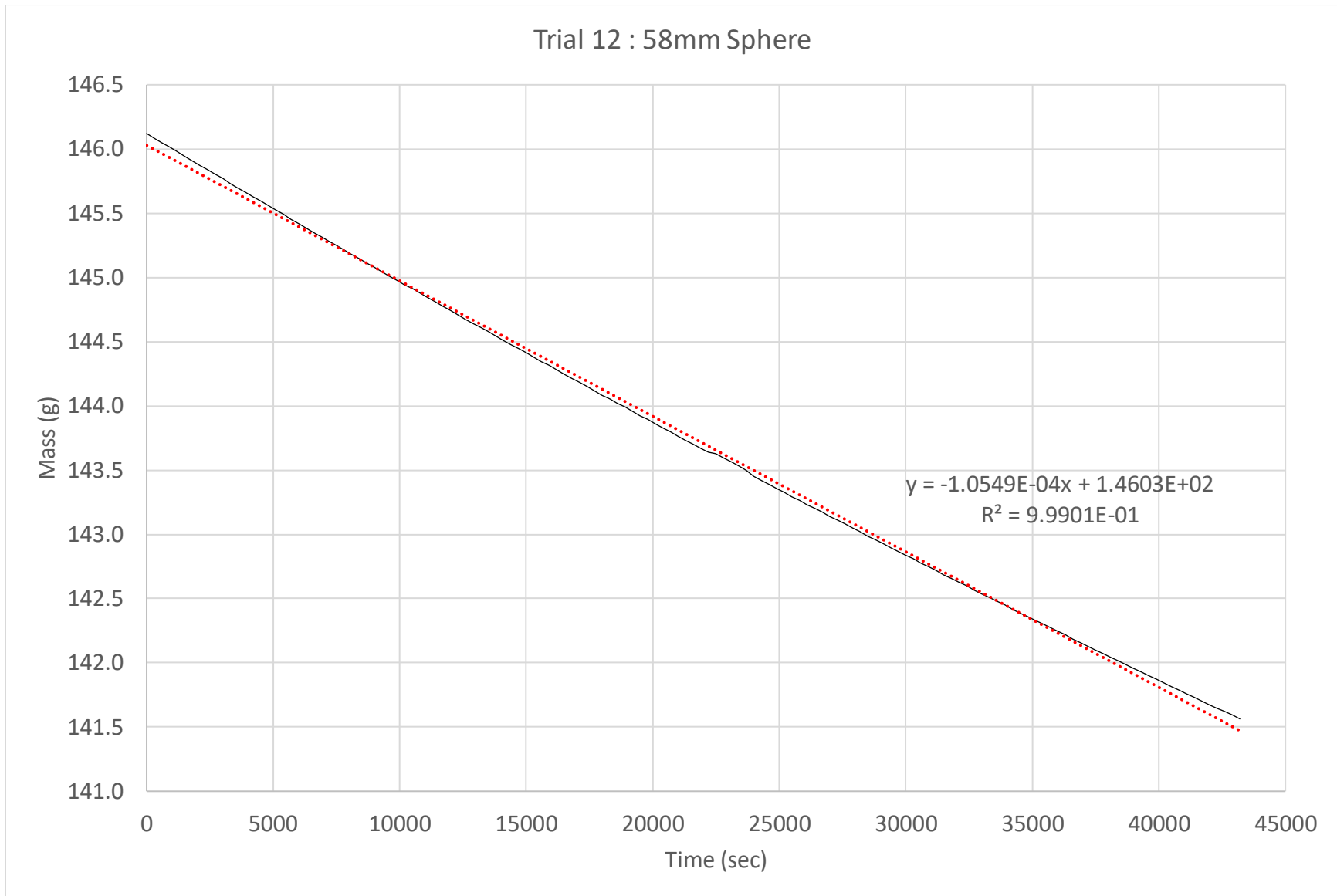


Figure 39: Experimental mass transfer rate plotted for trial 12.